Numerical study of two dimensional stochastic NLS equations

Marc Barton-Smith, Arnaud Debussche, Laurent Di Menza

Numerical study of two dimensional stochastic NLS equations

Marc BARTON-SMITH*, Arnaud DEBUSSCHE† and Laurent DI MENZA‡

∗ : CERMICS, ENPC, Cité Descartes, 77455 Champ-sur-Marne
† : ENS Cachan, Antenne de Bretagne, Campus de Ker-Lann, 35170 Bruz
‡ : Analyse Numérique et EDP, Université Paris-Sud, 91405 Orsay

Abstract: In this paper, we numerically solve the two-dimensional stochastic nonlinear Schrödinger equation in the case of multiplicative and additive white noises. The aim is to investigate their influence on well-known deterministic solutions: stationary states and blowing-up solutions. In the first case, we find that a multiplicative noise has a damping effect very similar to diffusion. However, for small amplitudes of the noise, the structure of solitary state is still localized. In the second case, a local refinement algorithm is used to overcome the difficulty arising for the computation of singular solutions. Our experiments show that multiplicative white noise stops the deterministic blow-up which occurs in the critical case. This extends the results of [15] in the one-dimensional case.

Keywords: Stochastic partial differential equations, multiplicative and additive noise, nonlinear Schrödinger equations, finite difference schemes, refinement procedure.

1 Introduction

Nonlinear Schrödinger equations (NLS) play an important role for the understanding of many physical phenomena. For instance, NLS appears in wave propagation in nonlinear media, fluid and quantum mechanics or plasma physics. It is well known that in some cases – in particular in the case of a focusing power law nonlinearity – NLS equations possess solutions of special form which are localized in space, propagating at a finite constant velocity and keeping the same shape. These are called solitary waves and in the particular case of a vanishing velocity these are called stationary waves (see [10] and [29] for a review on NLS). Depending on the power of the nonlinearity, these solitary waves are stable or unstable. Under a critical value of the nonlinear exponent, the nonlinearity is called subcritical and in this case, the solitary waves are stable. For larger values (that is in the critical and supercritical

cases), the solitary waves become unstable and the time evolution may exhibit blow-up.

In this paper, we wish to investigate the influence of different kinds of noises on solitary wave propagation and on the blow-up mechanism, in the two-dimensional case. Noisy terms might represent the effects of inhomogeneities in the medium in which the waves propagate, as well as noisy sources or of neglected terms in the modelization yielding to NLS equations. They can also be considered as a model of perturbation and it is natural to investigate if the qualitative behaviors described above are robust or not and how noise can change them. Here two different types of noises will be studied: additive noise and multiplicative noise. The first one acts as an additive random forcing term added to the NLS equation and has the form $i\epsilon\frac{dW}{dt}$; the case of additive noise is studied in [18] where collective coordinates and large deviation arguments are used to get information on the influence of the noise on the propagation of solitary waves. The second one can be seen as a random potential term of the form $i\epsilon u \circ \frac{dW}{dt}$ added to NLS equation. Multiplicative noise has been introduced in the context of Scheibe aggregates (see [5] and [27]). Then NLS is written as

$$du - i\Delta_d u\, dt - i|u|^{2\sigma}u\, dt = \begin{cases} i\epsilon u \circ dW \\ \\ i\epsilon dW, \end{cases} \tag{1}$$

where $u = u(t, x, w)$; $t \geq 0$ being the time variable, x the space variable and ω the random variable.

There are several studies on noisy nonlinear dispersive equations. In [23] for example, thanks to inverse scattering and perturbation techniques, the authors derive some qualitative informations for small noise for different equations like NLS, Korteweg-de Vries, Sine-Gordon or Klein-Gordon. The relevance of numerical simulations is also pointed out to obtain some results for more general noises. Such simulations have been used in [16] and [28] to study the influence of a white noise on the Korteweg-de Vries equation. NLS equations with random terms are described in [1], [2] and [19] (see also the references therein). In these articles, the noise is either a potential or a perturbation of the dispersive term or the nonlinear coefficient, it has smooth paths and again an inverse scattering transform is used. A numerical study of the influence of a noise on the blow-up for NLS has been performed in [15] in the case of a white noise in space dimension one. Furthermore, many theoretical results exist about the stochastic NLS (see for instance [11]) but valid only for correlated additive or multiplicative noises.

In this article, we want to do a similar study as in [15] in dimension two. We first recall, in Section 2, some basic concepts such as the stochastic framework and general well-posedness theoretical results. We also present the finite differences numerical method, emphasizing on the noise discretization. In Section 3, we study the effects of both additive and multiplicative noises on stationary waves in the subcritical and

critical cases. Let us recall that, in the case of space dimension two considered here, the physical model corresponds to the critical case, $\sigma = 1$, and the stationary wave is not stable. It results that the propagation can be studied only on a short time interval. Thus, we have chosen to simulate also a subcritical nonlinearity - $\sigma = 1/2$ - allowing the propagation over long time interval. We find that multiplicative noise has a damping effect that can be compared for large times with the damping observed for Ginzburg-Landau models. In Section 4, we numerically investigate the noise influence on blow-up formation in the critical case. Only multiplicative noise will be considered here, since additive noise has no real effect on the blow-up. Even for the deterministic case, the numerical method has to be consistent with small spatial scales of the blow-up structure. A local refinement algorithm is given, similar to the one given in [15] in the one-dimensional case, and tested first for deterministic blow-up. Refinement criteria have to give reasonable computational costs in our two-dimensional experiments. Note that a lot of works for the computation of the blow-up of deterministic NLS (see [3], [4], [29], [30] and [31]) or Korteweg-de Vries have been done ([7], [8]). Even if they concern deterministic equations and are based on finite elements, they are very helpful to find the correct techniques to compute blow-up in our stochastic cases. Stochastic tests are finally performed with different kinds of blowing-up solutions. The two dimensional case studied here is much more difficult than the one dimensional case studied in [15], especially for the computation of singular solutions. Indeed, the refinement method is much more difficult to derive here. Bad criteria for refinements yield expensive computational costs or very poor results. In Section 4, we try to give details on the difficulties encountered and the remedies we found. Moreover, the blow-up is much more severe in dimension two and it is difficult to detect the effect of a noise. We expect that a multiplicative noise always prevents the formation of singularities. However, if the blow-up is too strong we first have to simulate a strongly focusing solution reaching very high amplitudes and in some cases we have not been able to establish this fact.

2 General considerations on the equations and on the numerical scheme

2.1 Set up of the problem

The equations which will be studied here are the following:

$$\begin{cases} du - i\Delta_d u\, dt - i|u|^{2\sigma} u\, dt = \begin{cases} i\epsilon u \circ dW \\ i\epsilon dW, \end{cases} \\ u(0) = u_0. \end{cases} \tag{2}$$

Dirichlet boundary conditions will be considered on a square domain D of $\mathbb{R}^2$, u_0 is the initial condition, W is a real valued Wiener process on $L^2(D)$ associated with a filtered probability space $(\Omega, \mathcal{F}, \mathbb{P}, \{\mathcal{F}_t\}_{t\geq 0})$. The first kind of noise is referred as the

multiplicative case, where $i\epsilon u \circ dW$ has to be understood as a Stratonovitch product (see [5]), whereas the second one is referred as the additive case. When the noise W is a *cylindrical* Wiener process, it can be written as

$$W(t,x,\omega) = \sum_{k=0}^{\infty} \beta_k(t,\omega) e_k(x), \qquad t \geq 0,\, x \in D,\, \omega \in \Omega. \tag{3}$$

where $(\beta_k)_{k\in\mathbb{N}}$ are real independent brownian motions $(\beta_k)_{k\in\mathbb{N}}$ and $(e_k)_{k\in\mathbb{N}}$ is an orthonormal Hilbert basis of $L^2(D)$.

More generally, for a linear operator Φ on $L^2(D)$, a Wiener process with covariance operator Φ is given by

$$\Phi W(t,x,\omega) = \sum_{k=0}^{\infty} \beta_k(t,\omega) \Phi e_k(x), \qquad t \geq 0,\, x \in D,\, \omega \in \Omega.$$

In general, the series above do not converge in $L^2(D)$. This is true only when Φ is a Hilbert-Schmidt operator.

If Φ is defined through a kernel K

$$\Phi u(x) = \int_D K(x,y) u(y) dy, \quad \text{for} \quad u \in H,$$

then the spatial correlation function is given by:

$$C_\Phi(x,y) = \int_D K(x,z) K(z,y) dz.$$

The space and time correlation of ΦW being formally given by $\mathbb{E}\left[\left(\Phi\frac{dW}{dt}(t,x), \Phi\frac{dW}{dt}(s,y)\right)\right]$ and, still formally, we have:

$$\mathbb{E}\left[\left(\Phi\frac{dW}{dt}(t,x), \Phi\frac{dW}{dt}(s,y)\right)\right] = C_\Phi(x,y)\delta_{t-s}.$$

We see that this type of noise is always uncorrelated - or white - in time. If $\Phi = I_d$, *i.e.* if W is a cylindrical Wiener process, the noise is also white in space and the spatial correlation $C_\Phi(x,y)$ is the Dirac mass δ_{x-y}.

The correlation function is a physically measurable quantity; a correlation which is the Dirac mass $\delta_{x-y}\delta_{t-s}$ indicates a white noise both in time and space.
Let us also remark that it is often written $\dot{\eta} = \frac{d\Phi W}{dt}$ so that equation (2) becomes:

$$\frac{du}{dt} - i\Delta_d u - i|u|^{2\sigma}u = \begin{cases} i\epsilon u \circ \dot{\eta} \\ \\ i\epsilon\dot{\eta}. \end{cases} \tag{4}$$

For NLS, the energy and mass are respectively defined by:

$$H(u) = \frac{1}{2}\int_D \|\nabla u(x)\|^2 dx - \frac{1}{2(\sigma+1)}\int_D |u(x)|^{2(\sigma+1)} dx,$$

$$M(u) = \int_D |u(x)|^2 dx.$$

It is well-known (see for example [29]) that these quantities are invariant for the deterministic NLS. With an additive noise, none of them is conserved. For a Stratonovitch multiplicative noise, only the mass is conserved.

2.2 Main theoretical results

We think that it is important to recall the theoretical results on the NLS equation. Hopefully, this enables the reader to understand the issue at stake. We begin with the deterministic NLS equation.

Theorem 2.1. *For $u_0 \in H^1(\mathbb{R}^d)$, the deterministic NLS equation (that is $\epsilon = 0$) on $D = \mathbb{R}^d$ is locally well-posed if $0 \leq \sigma < \frac{2}{d-2}$ for $d > 2$ or for any σ if $d = 1$ or 2. Besides the solution is global if $\sigma d < 2$. Moreover, for $\sigma d \geq 2$ and $u_0 \in H^1(\mathbb{R}^d)$ such that $H(u_0) < 0$ and $xu_0 \in L^2(\mathbb{R}^d)$, then the solution blows-up at a finite time.*

The proof of this result as well as many improvements can be found in [10] and [29]. Note that if $\sigma d \geq 2$ there also exist solutions such that $H(u_0) > 0$ but blow up in a finite time. For evident reasons, it is not possible to simulate the NLS equation on $\mathbb{R}^d$ and we have to restrict our computations to a bounded domain. However, if we only simulate spatially localized solutions and the computational domain D is sufficiently large, we expect that the numerical solution is very close to the solution on $\mathbb{R}^d$. Another point is that in the case $d = 2$ considered in this article, it can be shown that in the subcritical case the NLS equation admits a unique global solution on bounded star-shaped domains (see [9]). Moreover, Kavian has shown in [22] that an initial data with negative energy on a star-shaped domain with Dirichlet condition also gives a blowing-up solution in the critical and supercritical cases.

For the NLS equations with additive noise $i\epsilon\Phi dW$, with Φ a Hilbert-Schmidt operator from $L^2(\mathbb{R}^d)$ to $H^1(\mathbb{R}^d)$, we have the following theorem, proved in [11, 12]:

Theorem 2.2. *Assume that $0 \leq \sigma < \frac{2}{d-2}$ if $d > 2$ or $0 \leq \sigma$ if $d \leq 2$. If u_0 is a $\mathcal{F}_0$ measurable random variable with values in $H^1(\mathbb{R}^d)$, then there exists a unique solution $u(u_0, .)$ to NLS with additive noise with continuous $H^1(\mathbb{R}^d)$ valued paths. This solution is defined on a random interval $[0, \tau(u_0, \omega))$, where $\tau(u_0, \omega)$ is a stopping time such that we almost surely have $\lim_{t \to \tau(u_0,\omega)} |u(t)|_{H^1} = \infty$ or $\tau(u_0, \omega) = \infty$. If $\sigma d < 2$ then $\tau(u_0, \omega) = \infty$ almost surely. Moreover, if $\sigma d \geq 2$, then for any $u_0 \in H^1(\mathbb{R}^d)$ such that $xu_0 \in L^2(\mathbb{R}^d)$ and any $t > 0$*

$$\mathbb{P}(\tau(u_0) < t) > 0.$$

For multiplicative noise $i\epsilon u \circ \Phi dW$, we have to assume that Φ a Hilbert-Schmidt operator from $L^2(\mathbb{R}^d)$ to $H^1(\mathbb{R}^d)$ and also that Φ is γ-radonifying operator from H to $W^{1,\alpha}(\mathbb{R}^d)$ (with $\alpha > 2d$), then we have the following theorem (see [11, 14]):

Theorem 2.3. *Assume that* $\frac{1}{2} < \sigma < \frac{2}{d-2}$ *or* $\sigma < \frac{1}{d-1}$ *if* $d > 3$, *or* $0 < \sigma < 2$ *if* $d = 3$, *or* $0 < \sigma$ *if* $d = 1$ *or* 2, *then there exist* $r \geq 2$ *and* p *be such that* $\frac{2}{r} = d(\frac{1}{2} - \frac{1}{p})$ *and for any* u_0 *with values in* $H^1(\mathbb{R}^d)$ *there exists a stopping time* $\tau(u_0, \omega)$ *and a unique solution of NLS with multiplicative noise starting from* u_0 *which is almost surely in* $\mathcal{C}([0,T], H^1(\mathbb{R}^d)) \cap L^r((0,T), W^{1,p}(\mathbb{R}^d))$ *for any* $T < \tau$. *Moreover we almost surely have:* $\limsup_{t \to \tau(u_0,\omega)} |u(t)|_{H^1} = \infty$ *or* $\tau(u_0, \omega) = \infty$. *If* $\sigma d < 2$ *then* $\tau(u_0, \omega) = \infty$ *almost surely. Moreover, if* $\sigma d > 2$ *and* Φ *is Hilbert-Schmidt from* $L^2(\mathbb{R}^d)$ *to* $H^2(\mathbb{R}^d)$, *then for any* $u_0 \in H^2(\mathbb{R}^d)$ *such that* $|x|^2 u_0 \in L^2(\mathbb{R}^d)$ *and any* $t > 0$

$$\mathbb{P}(\tau(u_0) < t) > 0.$$

If $\sigma d = 2$, *for* u_0 *as above with sufficiently negative energy, there exists* $\bar{t} > 0$ *such that*

$$\mathbb{P}(\tau(u_0) < \bar{t}) > 0.$$

Again, these results do not correspond with our situation since our simulations will be performed on a bounded domain. However, we think that the results presented below give a good idea of the behavior of the solutions of NLS equations on $\mathbb{R}^2$.

Note that, the noise has a strong effect on the blow-up mechanism. Contrary to the deterministic situation, in the supercritical case, any initial data gives a singular solution. This is also true in the critical case with additive noise. However, this assumes a spatially smooth noise. We will see in Section 4 that if the noise is white in space, the situation is completely different.

2.3 The numerical method

Our scheme is based on a Crank-Nicolson finite difference scheme in space and time on a uniform grid with $(M+1)^2$ points on the square domain $[0, x_{max}]^2$. This implicit scheme was chosen because the energy and the mass are conserved in deterministic case (see below for the definition of the numerical energy and mass). The time step is δt and u^n is the numerical solution at the discrete time $n\delta t$. The step of the square grid is h and $u_{k\,j}$ is the numerical solution at the point (kh, jh). The numerical scheme is the following:

$$\begin{aligned} i\frac{u_{k\,j}^{n+1} - u_{k\,j}^{n}}{\delta t} &+ \frac{1}{2h^2}\big((u_{k+1\,j}^{n+1} - 2u_{k\,j}^{n+1} + u_{k-1\,j}^{n+1} + u_{k+1\,j}^{n} - 2u_{k\,j}^{n} + u_{k-1\,j}^{n}) \\ &+ (u_{k\,j+1}^{n+1} - 2u_{k\,j}^{n+1} + u_{k\,j-1}^{n+1} + u_{k\,j+1}^{n} - 2u_{k\,j}^{n} + u_{k\,j-1}^{n})\big) + NL_{k\,j}^{n+\frac{1}{2}} \\ &= -\epsilon W_{k\,j}^{n+\frac{1}{2}} \end{aligned}$$

where

$$NL_{k\,j}^{n+\frac{1}{2}} = \frac{1}{2(\sigma+1)} \left(\frac{|u_{k\,j}^{n+1}|^{2\sigma+2} - |u_{k\,j}^{n}|^{2\sigma+2}}{|u_{k\,j}^{n+1}|^2 - |u_{k\,j}^{n}|^2} \right) \left(u_{k\,j}^{n+1} + u_{k\,j}^{n}\right)$$

and

$$W_{k\,j}^{n+\frac{1}{2}} = \begin{cases} \dfrac{1}{2h\sqrt{\delta t}} w_{k\,j}^{n+\frac{1}{2}} (u_{k\,j}^{n+1} + u_{k\,j}^{n}) & \text{for multiplicative noise} \\ \\ \dfrac{1}{h\sqrt{\delta t}} w_{k\,j}^{n+\frac{1}{2}} & \text{for additive noise.} \end{cases} \tag{5}$$

The $w_{k\,j}^{n+\frac{1}{2}}$ are independent real normal random variables. Actually, for additive an delta correlated - or equivalently a space-time white - noise, this numerical noise $W_{k\,j}^{n+\frac{1}{2}}$ should be the approximation of

$$\frac{1}{h^2 \delta t} \int_{D_{k\,j}} \int_{n\delta t}^{(n+1)\delta t} dW dx, \tag{6}$$

where $D_{k\,j}$ is the elementary square domain around $x_{k\,j}$ given by

$$D_{k\,j} = \left[(k - \frac{1}{2})h \, , \, (k + \frac{1}{2})h \right] \times \left[(j - \frac{1}{2})h \, , \, (j + \frac{1}{2})h \right].$$

Then with the definition (3) of Section 2.1 we get,

$$\begin{aligned} \frac{1}{h^2 \delta t} \int_{D_{k\,j}} \int_{n\delta t}^{(n+1)\delta t} dW dx &= \frac{1}{h^2 \delta t} \int_{D_{k\,j}} \int_{n\delta t}^{(n+1)\delta t} \sum_{m \in \mathbb{N}} e_m(x) d\beta_m(s) dx \\ &= \frac{1}{h^2 \delta t} \sum_{m \in \mathbb{N}} \left(\int_{D_{k\,j}} e_m(x) dx \right) \int_{n\delta t}^{(n+1)\delta t} d\beta_m(s). \end{aligned}$$

Let us choose the Hilbert basis such that the e_m are the functions $e_{k\,j} = \frac{1}{h} \chi_{D_{k\,j}}$ vanishing outside $D_{k\,j}$, completed by an infinite number of functions in order to have a Hilbertian basis. Then by orthogonality, we have

$$\int_{D_{k\,j}} e_{l,m}(x) dx = 0$$

if $(l, m) \neq (k, j)$ and we get

$$\begin{aligned} \frac{1}{h^2 \delta t} \int_{D_{k\,j}} \int_{n\delta t}^{(n+1)\delta t} dW dx &= \frac{1}{h^2 \delta t} \left(\int_{D_{k\,j}} e_{k\,j}(x) dx \right) \int_{n\delta t}^{(n+1)\delta t} d\beta_{k\,j}(s) \\ &= \frac{1}{h \delta t} \int_{n\delta t}^{(n+1)\delta t} d\beta_{k\,j}(s) \qquad (7) \\ &= \frac{1}{h \delta t} (\beta_{k\,j}((n+1)\delta t) - \beta_{k\,j}(n\delta t)). \qquad (8) \end{aligned}$$

Since $(\beta_m((n+1)\delta t)-\beta_m(n\delta t))/\sqrt{\delta t}$ is a random variable with normal law $\mathcal{N}(0,1)$, it can be set $w_{k\,j}^{n+\frac{1}{2}} = (\beta_{k\,j}((n+1)\delta t)-\beta_{k\,j}(n\delta t))/\sqrt{\delta t}$, so that the numerical stochastic term becomes

$$W_{k\,j}^{n+\frac{1}{2}} = \frac{1}{h\sqrt{\delta t}} w_{k\,j}^{n+\frac{1}{2}},$$

where the random variables $w_{k\,j}^{n+\frac{1}{2}}$ are simulated thanks to an appropriate random procedure. Thus, we see that, in the additive case, the numerical noise is the exact projection of the space-time white noise. However it is not delta correlated and it is only an approximation of the white noise. Indeed it is easily seen that the numerical noise corresponds also to the projection of $\epsilon\Phi_{num}dW$, where Φ_{num} is the orthogonal projector onto the space spanned by $(e_{k\,j})_{(k,j)\in[1,M-1]^2}$. In other words we also have:

$$\begin{aligned}
\frac{1}{h^2\delta t}\int_{D_{k\,j}}\int_{n\delta t}^{(n+1)\delta t} \Phi_{num}dWdx &= \frac{1}{h^2\delta t}\sum_{m\in\mathbb{N}}\left(\int_{D_{k\,j}}\Phi_{num}e_m(x)dx\right)\int_{n\delta t}^{(n+1)\delta t} d\beta_m(s) \\
&= \frac{1}{h^2\delta t}\sum_{(k,j)\in[1,n-1]^2}\left(\int_{D_{k\,j}} e_{k\,j}(x)dx\right)\int_{n\delta t}^{(n+1)\delta t} d\beta_m(s).
\end{aligned}$$

The numerical noise space correlation is $C_{num}(x,y) = \frac{1}{h^2}$ if x and y belong to the same $D_{k\,j}$ and $C_{num}(x,y) = 0$ otherwise. This is only an approximation of the Dirac mass $\delta(x-y)$.

For multiplicative noise the approximation of the numerical noise is similar. However the stochastic integral is calculated with two different methods for Ito noise and Stratonovitch noise. Starting from (7), we can approximate the stochastic Ito integral by:

$$\begin{aligned}
\int_{n\delta t}^{(n+1)\delta t} u(x_{k\,j},s)d\beta_{k\,j}(s) &\simeq u(x_{k\,j},n\delta t)(\beta_{k\,j}((n+1)\delta t)-\beta_{k\,j}(n\delta t)) \\
&\simeq u_{k\,j}^n w_{k\,j}^n\sqrt{\delta t},
\end{aligned}$$

which follows the definition of an Ito product, whereas for a Stratonovitch integral, we have

$$\begin{aligned}
\int_{n\delta t}^{(n+1)\delta t} u(x_{k\,j},s)\circ d\beta_{k\,j}(s) &\simeq \frac{1}{2}\big(u_{k\,j}^n + u_{k\,j}^{n+1}\big)(\beta_{k\,j}((n+1)\delta t)-\beta_{k\,j}(n\delta t)) \\
&\simeq \frac{1}{2}\big(u_{k\,j}^n + u_{k\,j}^{n+1}\big) w_{k\,j}^{n+\frac{1}{2}}\sqrt{\delta t},
\end{aligned}$$

which corresponds to the approximation given in (5). It is well-known that the Stratonovitch product $u\circ dW$ has an Ito equivalent with a correction term $\frac{1}{2}iuF_\Phi$, where F_Φ only depends on the covariance operator, see [11]. But F_Φ is not well-defined for a space time white noise and what is more important, a discretization of this equivalent Ito equation would not keep the numerical mass M_n constant (see the

notation just below). Thus we have chosen to approximate directly the Stratonovitch product. The price to pay is that the random term is implicit.

If we denote by L the linear operator

$$(Lu)_{k\,j} = \frac{1}{2h^2}(u_{k+1\,j} - 2u_{k\,j} + u_{k-1\,j} + u_{k\,j+1} - 2u_{k\,j} + u_{k\,j-1}),$$

the nonlinear system

$$i\frac{u^{n+1} - 2u^n}{\delta t} + \frac{1}{2}L(u^{n+1} + u^n) + NL^{n+\frac{1}{2}} = -\epsilon W^{n+\frac{1}{2}}$$

has to be solved at each time step. The system can be rewritten as

$$\left(\frac{i}{\delta t}I + \frac{1}{2}L\right)u^{n+1} = \left(\frac{i}{\delta t}I - \frac{1}{2}L\right)u^n - \epsilon W^{n+\frac{1}{2}} - NL^{n+\frac{1}{2}} \tag{9}$$

and will be solved using a fixed point method. The matrix $M = \frac{1}{\delta t}I + \frac{1}{2}L$ does not depend on the unknown and is easy to invert. This is the reason for leaving the linear contribution of the noise in the right hand side in the multiplicative case. At each time step, a fixed point algorithm is used and the matrix M is inverted with a conjugated gradient method. Besides M is diagonally preconditioned before being inverted, which is often sufficient to fasten the calculation since the next time step solution is quite close to the previous time step solution. The iteration number for the convergence of the conjugated gradient remains small (less than 4 or 5 iterations for the gradient and the fixed point in all the subcritical cases).

It can be seen that system (9) has at least one solution u^{n+1} (see [13] in the semi discrete case). However, we do not know if it is unique and we have no guarantee that the iteration converges. In [24], it is proposed to avoid this problem by a cut-off of the simulated random variables. Since we never encountered any trouble of this type and the fixed point iteration always converges, we decided not to use this cut-off.

The numerical mass and energy are respectively given by

$$H^n = \frac{1}{2}\sum_{k\,j}(|u^n_{k\,j+1} - u^n_{k\,j}|^2 + |u^n_{k+1\,j} - u^n_{k\,j}|^2) - \frac{h^2}{2(\sigma+1)}\sum_{k\,j}|u^n_{k\,j}|^{2(\sigma+1)}$$
$$M^n = h^2\sum_{k\,j}|u^n_{k\,j}|^2$$

It is well-known that these discrete quantities are also numerically conserved in the case of the deterministic NLS with the scheme (9). In the case of a multiplicative noise the mass M^n also remains constant (see [15]).

In our stochastic computations, it is important to compute several trajectories in order to have an idea of the generic behavior of the solutions and to compute expectations. To compute an approximation of expectations of the solutions and other quantities, an average is made on 50 or 100 trajectories. This might seem not

sufficient, but each trajectory can take a certain time of computation. Therefore an accurate approximation of the expectation would require a very long computational time. This explains why the different curves of expectations shown below are not as smooth as they should be. Nevertheless an average computed on 50 or 100 trajectories gives a sufficient idea of what the expectation is. We use the notation $< \cdot >$ for the empirical average which approximates the mathematical expectation $\mathbb{E}(\cdot)$. For instance, if N is the number of computed trajectories, we have:

$$< |u(t, x_{k,j})| >= \frac{1}{N} \sum_{1 \leq \ell \leq N} |u^{\ell}_{k,j}(t)| \text{ and } |< u(t, x_{k,j}) >| = \frac{1}{N} \left| \sum_{1 \leq \ell \leq N} u^{\ell}_{k,j}(t) \right|$$

for the numerical approximation of the averaged amplitude $\mathbb{E}(|u(t,x)|)$ and the amplitude of the average $|\mathbb{E}(u(t,x))|$.

This scheme was coded in a C++ language, all the operations are guaranteed to be optimum. More details about this code, its UML diagram and the definitions of its elements, can be found in [6]. The Gaussian random variable $w^{n+\frac{1}{2}}_{k\,j}$ are simulated thanks to a random generator routine whose period is 10^{26} (©1993,4,6: R. B. Davies). For every n, k and j, the $w^{n+\frac{1}{2}}_{k\,j}$ are independent. This length of the period is sufficient to guarantee the independence of each random draw. Indeed the grid has a maximum of 500×500 points and the maximum number of time iterations in our simulations is 5000 and there were never more than 200 trajectories calculated to approach the average solution. In this worst case, the number of random draws is 250.10^9 which is still very small compared to the period.

Let us remark that, in the deterministic case, this scheme is known to be stable and consistent. It keeps the energy and mass conserved and is convergent of order 1 in time and 2 in space (see [21], [26]). Convergence results for the stochastic scheme are delicate to obtain. For the stochastic Schrödinger equation (see [13]), it has been proved that the numerical solution of the semi-discrete equation (time discrete equation) converges in probability in different spaces. The study of the fully discrete scheme is under progress.

Finally, we note that the strategy we use to simulate a white noise is not the only possibility. For instance, it would be possible to use a Fourier basis to define the Wiener process W. Then a Fast Fourier Transform would give the values of the noise in the spatial domain. In a forthcoming work, we will study the influence on the discretization of the noise on the numerical solutions.

Note also that a split step algorithm is often used to simulate NLS equations. However, it is known that these schemes do not respect the balance between diffractive and nonlinear effects and thus perturbs the propagation. We think that with such a scheme it would be difficult to understand the real effect of a noise on the propagation. We have preferred the Crank-Nicolson scheme, for which the problem does not occur.

3 Noise effects on Schrödinger stationary solitary waves

In this Section, we want to investigate the noise effects on stationary solutions in different cases. As mentioned in the introduction, stationary waves play an important role in physics and the effect of white noise on propagation is not well-known. Noise effects on solitary waves have already been studied for NLS equation and for Korteweg-de Vries equation (see [15], [16], [25], and [28]), these are equations in dimension one. Here we try to see if in dimension two a similar behavior is observed.

Two different types of solitary waves are going to be investigated: stationary (stable) waves in the subcritical case $\sigma = 0.5$, and stationary (unstable) waves in the critical case $\sigma = 1$. The stationary waves are given by the time-periodic solutions

$$u(x,t) = u_0(x)e^{i\omega t},\ \omega > 0,$$

where u_0 is a real valued function and is explicitly known in the case $d = 1$. For $d = 2$, it can be computed separately with a shooting method using Maple, assuming that the solution u_0 is radial (see [29] for further details). The period for this solution is then $T = \frac{2\pi}{\omega}$ and will be set to 2π (that is $\omega = 1$) in the following (see figure 1 for the stationary profile obtained with $d = 2$, $\sigma = 0.5$ and $\omega = 1$). The numerical tests will be made with various noise amplitudes ϵ.

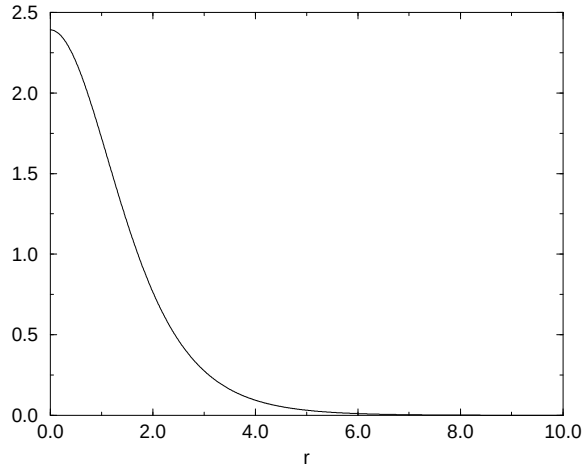

Figure 1: The stationary wave in the case $d = 2$, $\sigma = 0.5$ and $\omega = 1$.

3.1 Stationary solution in the subcritical case ($\sigma = \frac{1}{2}$)

The solution is stable and we can perform simulations on long time intervals. In our deterministic simulation, the solitary wave stays the same with a relative precision of 10^{-2} during a period and a half. Consequently we can consider that the deterministic solution is stationary for our simulations whose time calculations will not go over this limit $T = 3\pi$. The computations have been made on $D = [0, 14]^2$ with a uniform

grid 140×140, $\delta t = 5.10^{-3}$ and $\sigma = \frac{1}{2}$, with a stationnary state u_0 centered at the point $(7, 7)$.

We first look at the effect of noise on one trajectory. Figure 2 shows the profile of the solution with multiplicative (left) and additive (right) noise at different instants. The first observation is that the profile is not destroyed by the noise. However, as was already observed in dimension one, the multiplicative noise damps the profile: the final amplitude is clearly much smaller than the initial amplitude. On the contrary, the amplitude of the solution seems to oscillate with additive noise If the noise level is increased, we see on figure 3 that the damping effect in the multiplicative case is really strong and the wave has been completely destroyed at time 10. But, for additive noise, even with this very high level, the wave is still clearly there. Other solutions corresponding to other paths of the noise have been simulated and each time a similar behavior was observed. We recover here the strong stability of the propagation in the presence of an additive noise already observed in the case of the Korteweg-de Vries equation (see [16]).

With these long computations, the solution becomes non negligible at the boundary. Since we do not want boundary reflections to change the general behavior of the stationary wave, solutions in a larger domain (see figure 4) and solutions with periodic boundary conditions (see figure 5) have also been simulated. No major difference can be seen here for the solution of NLS with multiplicative noise. For additive noise no comparison are shown, but also in this case no real difference were observed. Moreover the comparisons of figures 5 are done with the same path of the noise and the same irregularities on the profiles can be observed. In addition to that, a few simulations were also done to compare Dirichlet and periodic boundary conditions on averages - such as $\mathbb{E}(\max_{x \in D} |u(t,x)|)$ or any other quantity studied below - and no relevant difference in the solution behavior could be observed. For these reasons, our next simulations will only be performed in the domain $[0, 14]^2$ with Dirichlet conditions and we think that this particular choice of boundary conditions does not have any effect on the general behavior.

Another way to understand the effect of a noise on the solutions of the NLS equation is to simulate average quantities, which corresponds to mathematical expectations. In order to keep a reasonable computational cost, only 100 trajectories were used to simulate these averages. This is not sufficient to have a good precision but it gives a good idea of the influence of a noise. In figure 6, we show the section across the x axis of the averaged amplitude $< |u| >$ at time 0 and $\pi/2$. The shape of the solitary wave is well conserved and the damping effect of the multiplicative noise is confirmed. Moreover, it is amplified when the level of noise is increased. It seems that the additive noise also has a damping effect however it is rather weak even with a very high noise level. Figure 7 shows the same quantity at time $T = 8$, the damping effect of the additive noise is now clear. This effect has been called "soliton diffusion" in the context of the Korteweg-de Vries equation (see [28]) and can be justified in some cases (see [23]).

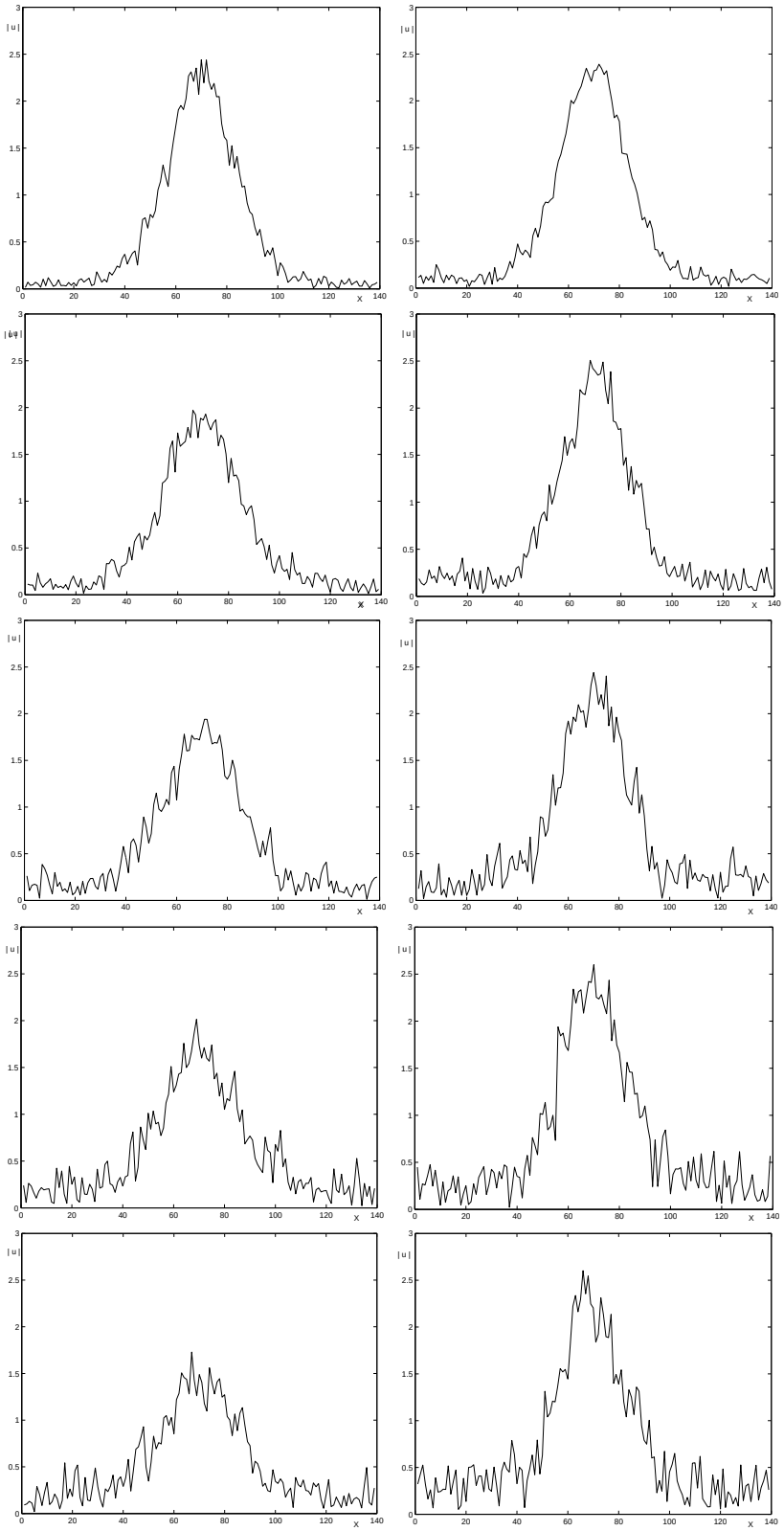

Figure 2: Evolution of the sections at times $t = 2,\ 4,\ 6,\ 8,\ 10$ for NLS with multiplicative noise (left) and with additive noise (right), ($\sigma = \frac{1}{2}$, $\epsilon = 0.03$).

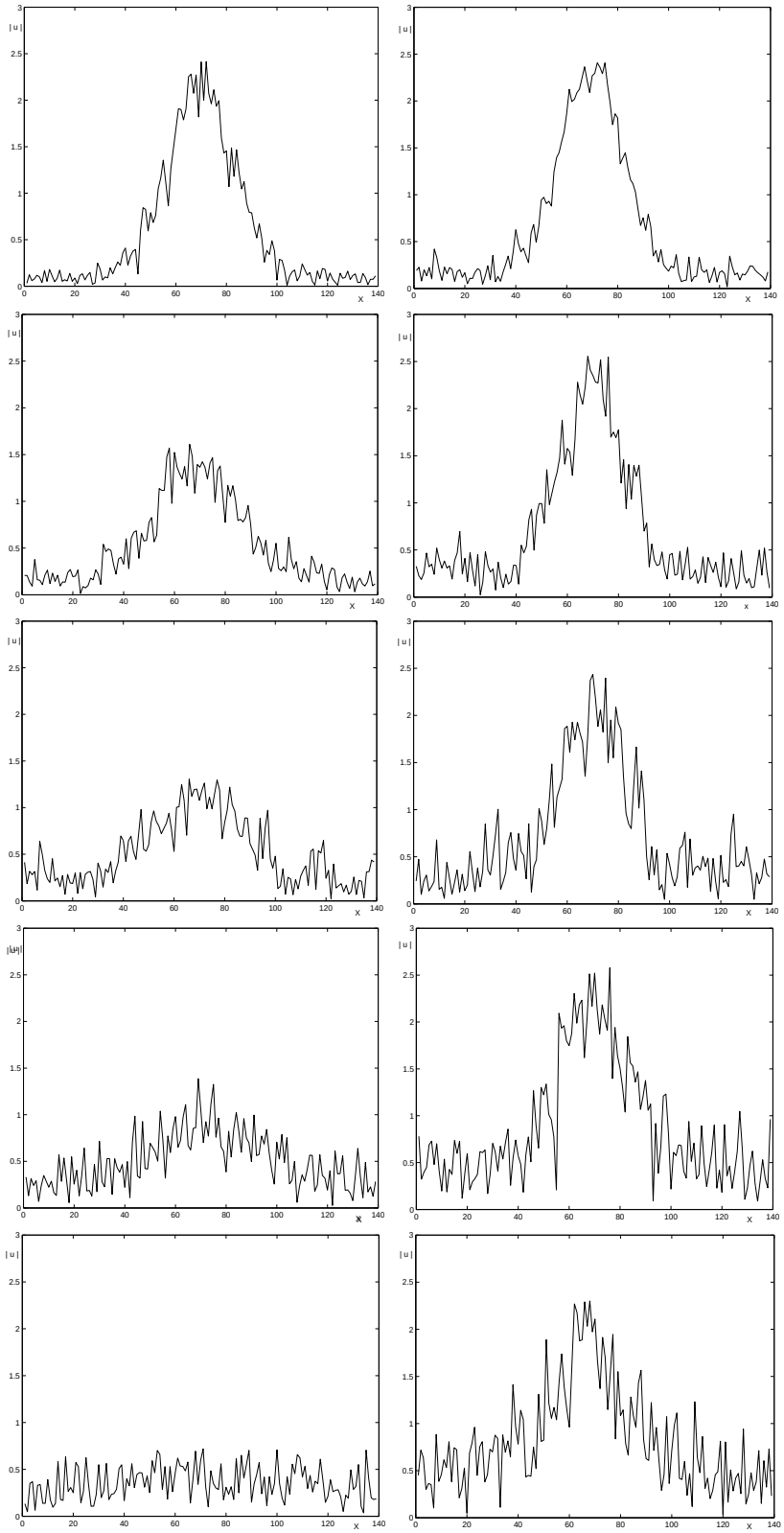

Figure 3: Evolution of the sections at times $T = 2,\ 4,\ 6,\ 8,\ 10$ for NLS with multiplicative noise (left) and additive noise (right), ($\sigma = \frac{1}{2}$, $\epsilon = 0.05$).

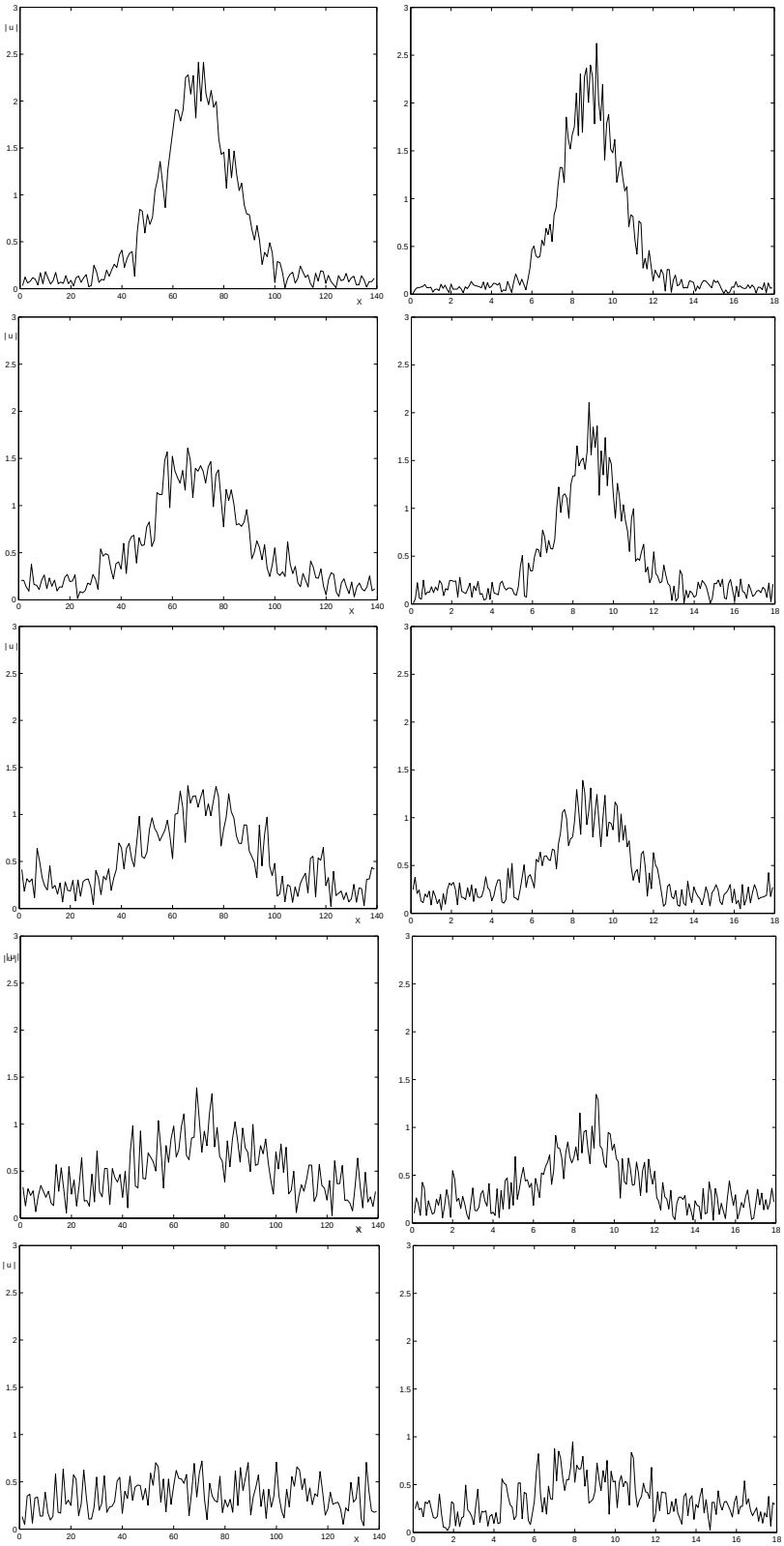

Figure 4: Evolution of the sections at times $t = 2,\ 4,\ 6,\ 8,\ 10$ for NLS with multiplicative noise with Dirichlet boundary conditions on $[0, 14]$ (left) and $[0, 18]$ (right) ($\sigma = \frac{1}{2}$, $\epsilon = 0.05$, $h = 0.1$).

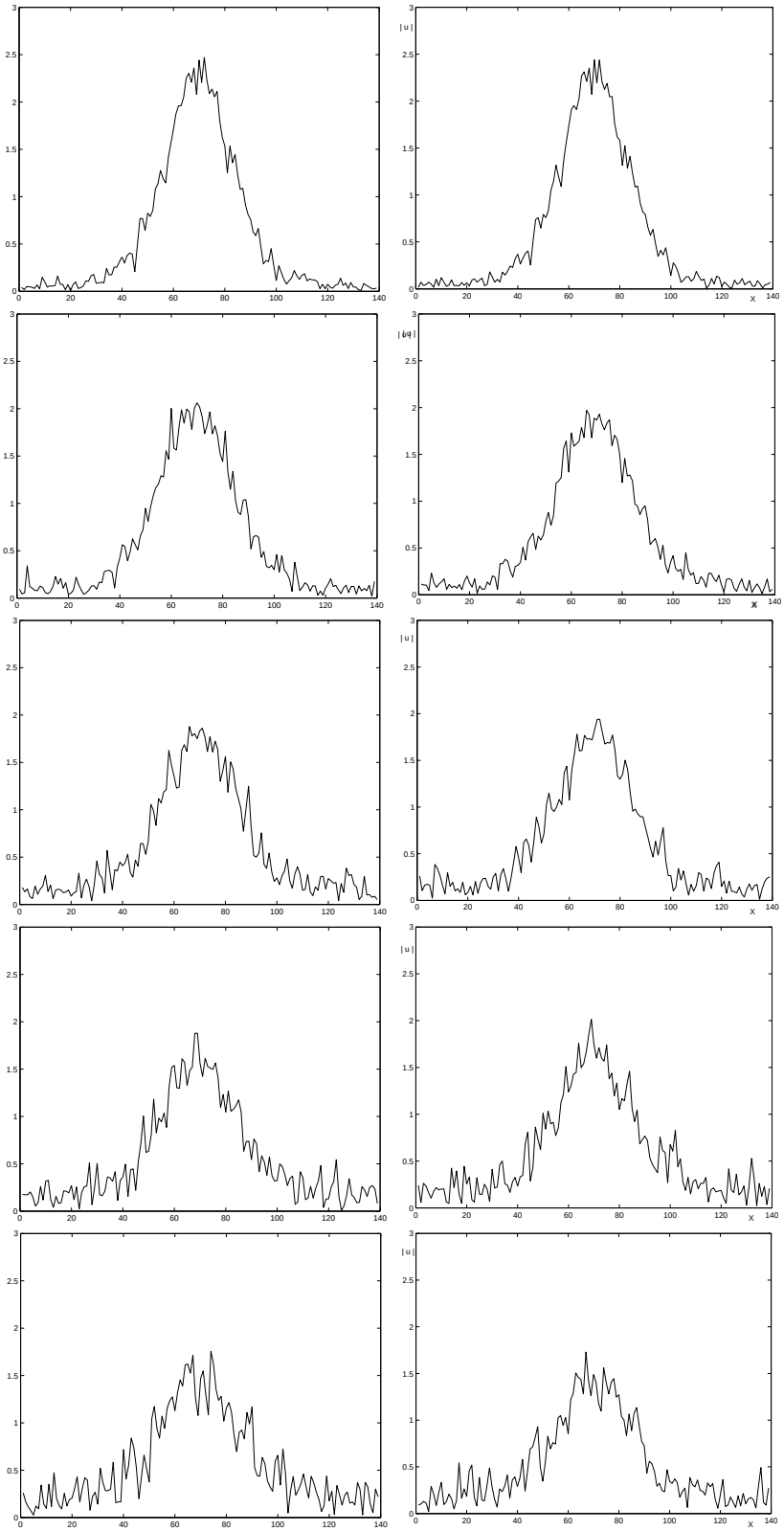

Figure 5: Evolution of the sections at times $t = 2,\ 4,\ 6,\ 8,\ 10$ for NLS with multiplicative noise with Dirichlet (left) and periodic (right) boundary conditions ($\sigma = \frac{1}{2}$, $\epsilon = 0.03$).

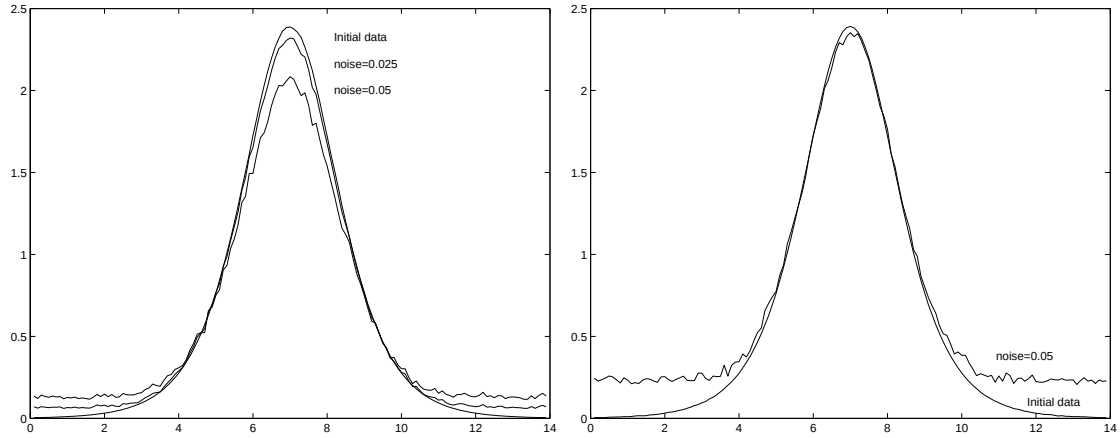

Figure 6: Average sections at $T = \frac{\pi}{2}$ for NLS with multiplicative (left) and additive (right) noise, ($\sigma = \frac{1}{2}$, $\epsilon = 0.05; 0.025$).

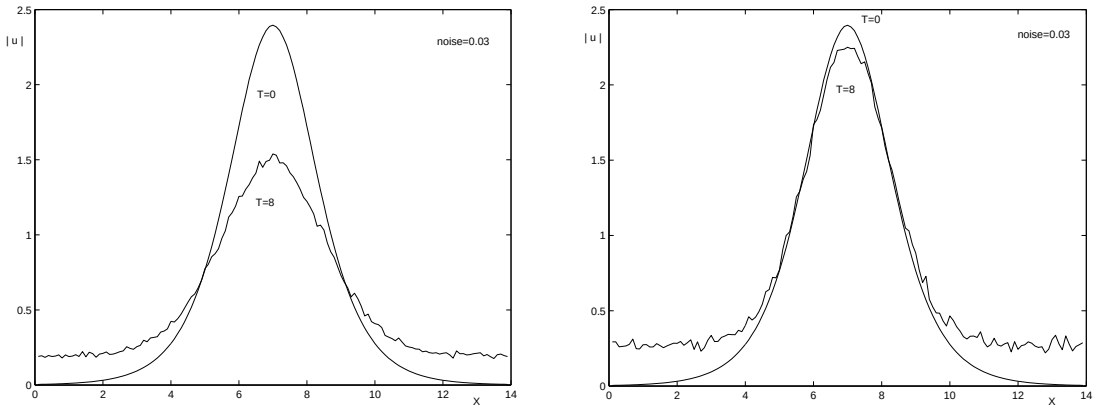

Figure 7: Comparison of the final section of $< |u(t,x)| >$ at different times for NLS with multiplicative (left) and additive (right) noise , ($\sigma = \frac{1}{2}$, $\epsilon = 0.03$).

We also see that $< |u| >$ does not vanish near the boundary. In fact, $< |u| >$ is constant outside the region where the wave is localized. This constant increases with ϵ and reflects the averaged amplitude of the background noise. If the amplitude of the average $| < u > |$ is computed instead of the average of the amplitude, $< |u| >$, we see on figure 8 that $| < u > |$ vanishes outside the solitary wave profile. This is due to the fact that the background noise has zero average. Except for this point, the two quantities behave similarly.

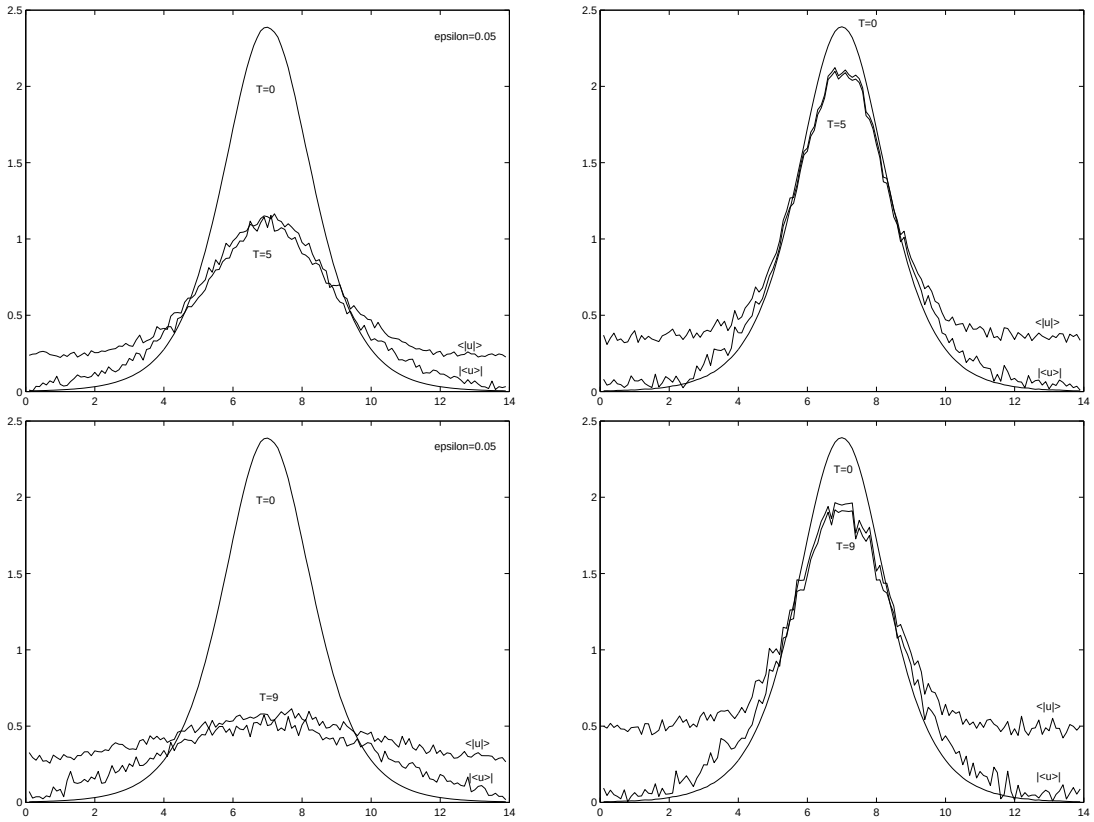

Figure 8: Comparison of the final section of $< |u(t,x)| >$ or $| < u(t,x) > |$ at time $T = 5$ and $T = 8$ for NLS with multiplicative (left) and additive (right) noise , ($\sigma = \frac{1}{2}$, $\epsilon = 0.05$).

We have seen that the maximum of the averaged amplitude decreases in both the multiplicative and additive case. We now investigate in more details this quantity $\max_{x\in D} \mathbb{E}(|u(t,x)|)$ and compare it to the average of the maximum $\mathbb{E}(\max_{x\in D} |u(t,x)|)$.

Figure 9 displays the evolution of these quantities as well as $\mathbb{E}(|u(t,x_c)|)$, x_c being the center of the domain. A first observation is that $\max_{x\in D} \mathbb{E}(|u(t,x)|)$ and $\mathbb{E}(|u(t,x_c)|)$ are very close and we deduce that $\mathbb{E}(|u(t,x_c)|)$ is a very good approximation of $\max_{x\in D} \mathbb{E}(|u(t,x)|)$. This is important since $\max_{x\in D} \mathbb{E}(|u(t,x)|)$ is naturally approximated by $\max_{k,j} < |u(t,x_{k,j})| >$ where $x_{k,j}$ are the grid points and the computation of this quantity requires to save $|u(t,x_{k,j})|$ for all points $x_{k,j}$ and for each time and for each trajectory. Thus, a lot of memory storage is necessary. In the following we often show the evolution of $\mathbb{E}(|u(t,x_c)|)$ which is cheaper to compute.

Also, we see that $\max_{x\in D} \mathbb{E}(|u(t,x)|)$ monotonically decreases. On the contrary, $\mathbb{E}(\max_{x\in D} |u(t,x)|)$ increases first on a small interval of time and then decreases for multiplicative noise and monotonically increases for additive noise. A possible explanation is that the noise has two effects: it injects energy and induces a damping. At the beginning, the injection of energy dominates because the damping mechanism is not settled. Then, after some time, the situation changes and the damping dominates in the multiplicative case. However, in the additive case, the damping is too weak and cannot counterbalance the injection of energy.

The injection of energy cannot be seen on $\mathbb{E}(|u(t,x_c)|)$, or on $\max_{x\in D}\mathbb{E}(|u(t,x)|)$, because it is injected at points which are random. When a point is fixed, the energy is injected there for very few trajectories so that it has no influence on the average. This explains why we obtain decreasing curves which only reflect the damping effect.

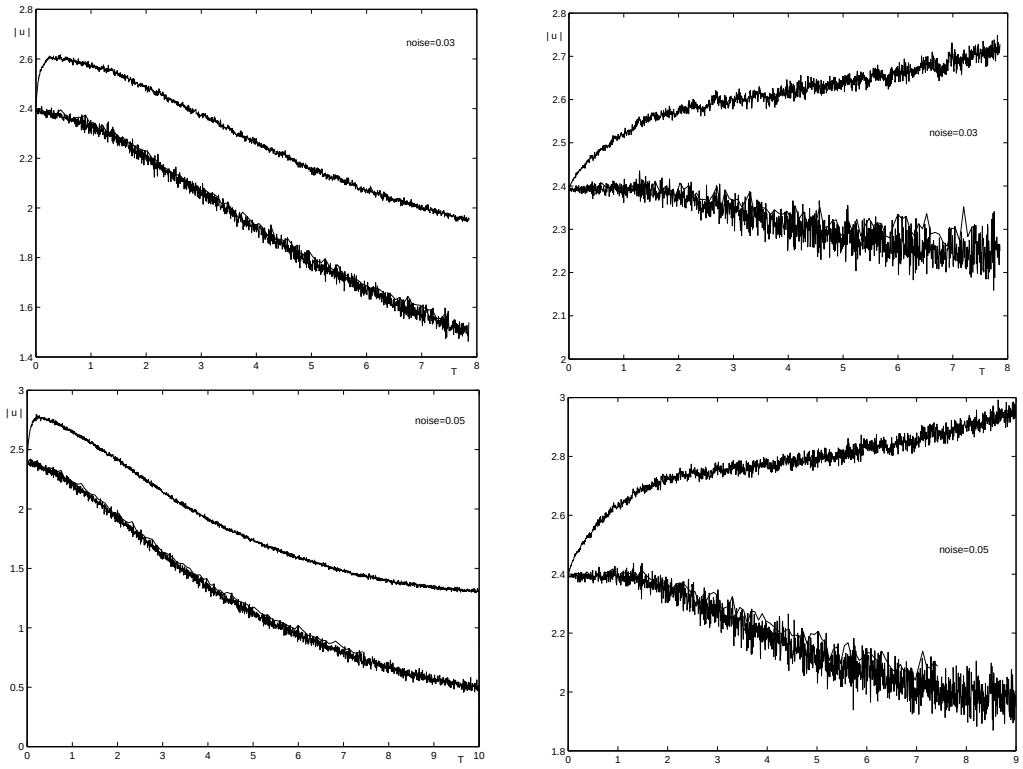

Figure 9: Evolutions of $\mathbb{E}[\max|u(t,x)|]$, $\max\mathbb{E}|u(t,x)|$ and $<|u(t,x_c)|>$ for NLS with multiplicative (left) and additive (right) noise , ($\sigma=\frac{1}{2}$, $\epsilon=0.03,\ 0.05$).

In [15, 16, 28, 23], the decrease of $\max_{x\in D}\mathbb{E}(|u(t,x)|)$ is referred as "soliton diffusion" and it is shown that for intermediate time it behaves like $t^{-\gamma}$ where γ does not depend on the noise level. In our two dimensional simulations, we have not been able to fit the observed decrease with $t^{-\gamma}$.

3.2 Stationary solution in the critical case

We now consider the critical case $\sigma=1$. Due to instability, in the deterministic case the solution is stationary with a good precision only on a quarter period, $T=\pi/2$. The solution amplitude is numerically constant with a relative precision of 10^{-2} on that interval, see figure 10. Afterwards instability effects dominate and the amplitude increases. Since, in this Section, we do not want to mix noise effects and instability, our simulations will be performed on this time interval $[0,\pi/2]$.

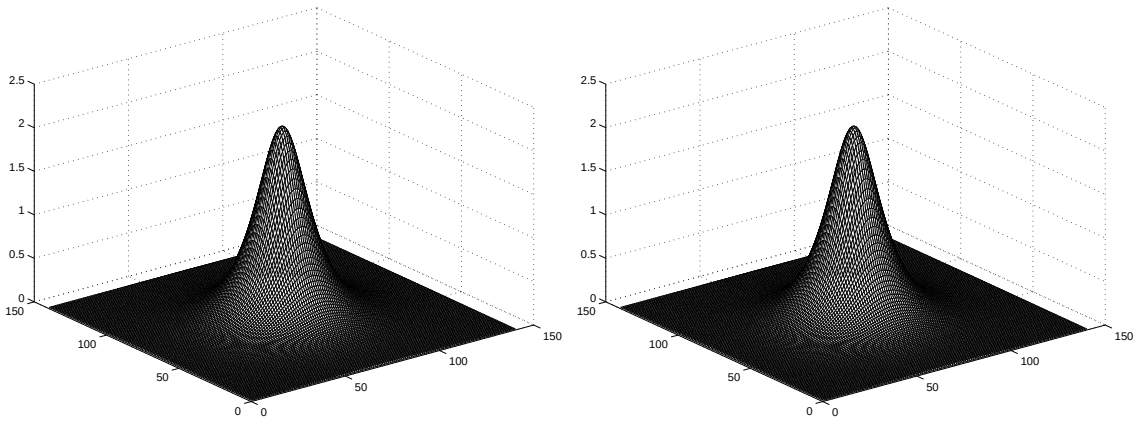

Figure 10: Initial Surface (left) and surface solution of deterministic NLS at $T = \pi/2$ (right), ($\sigma = 1$, $\epsilon = 0$).

The computational parameters are the following: the space domain is $\Omega =]0, 10[\times]0, 10[$, with a grid 140×140 and the number of time iterations is 314 with $\delta t = 5.10^{-3}$, corresponding to the final time limit close to T.

We first investigate the additive and multiplicative noise effect on a single trajectory. Figures 11 and 12 show the profile at $T = \pi/2$ with two different noise levels. The behavior is very similar to the subcritical case.

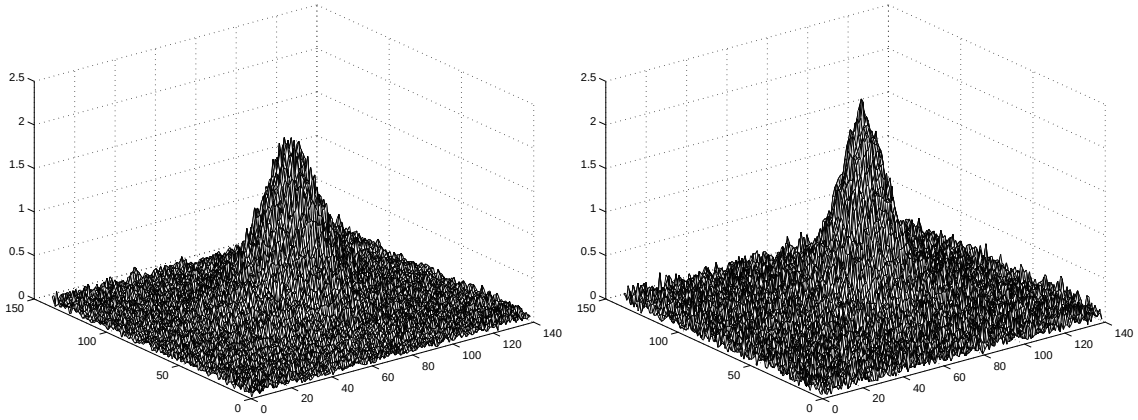

Figure 11: Surfaces solutions of stochastic NLS at $T = \pi/2$ for multiplicative noise (left) and additive noise (right) ($\sigma = 1$, $\epsilon = 0.025$).

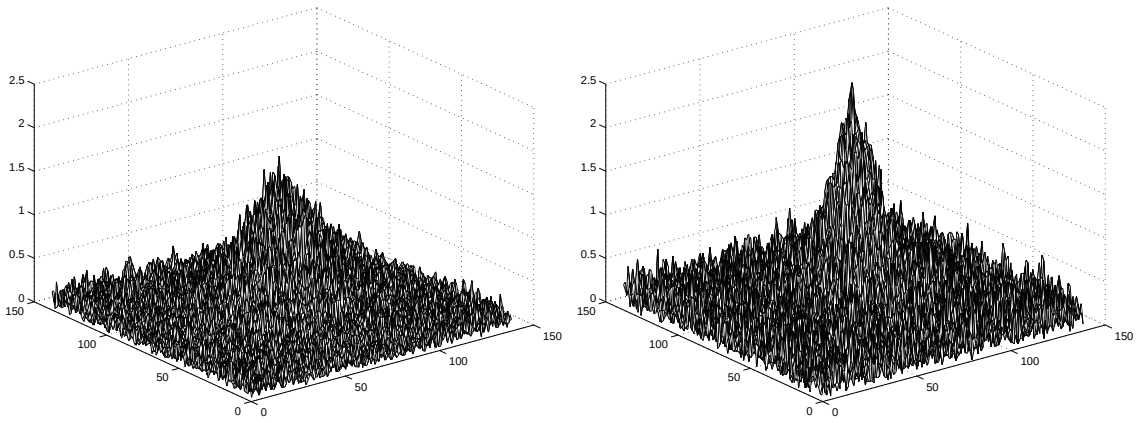

Figure 12: Surfaces solutions of stochastic NLS at $T = \pi/2$ for multiplicative noise (left) and additive noise (right) ($\sigma = 1$, $\epsilon = 0.05$).

In figure 13, we show the section across the x axis of the averaged amplitude $< |u| >$ after a quarter period. The shape of the solitary wave is again well conserved, even with a very high noise level such as $\epsilon = 0.05$. The paths in this case are really chaotic, see figure 12, but the averaged profile is a smooth curve.

The damping effect of the multiplicative noise is confirmed and it is clearly amplified when the level of noise is increased. On the contrary, the additive noise does not seem to have a significant effect here.

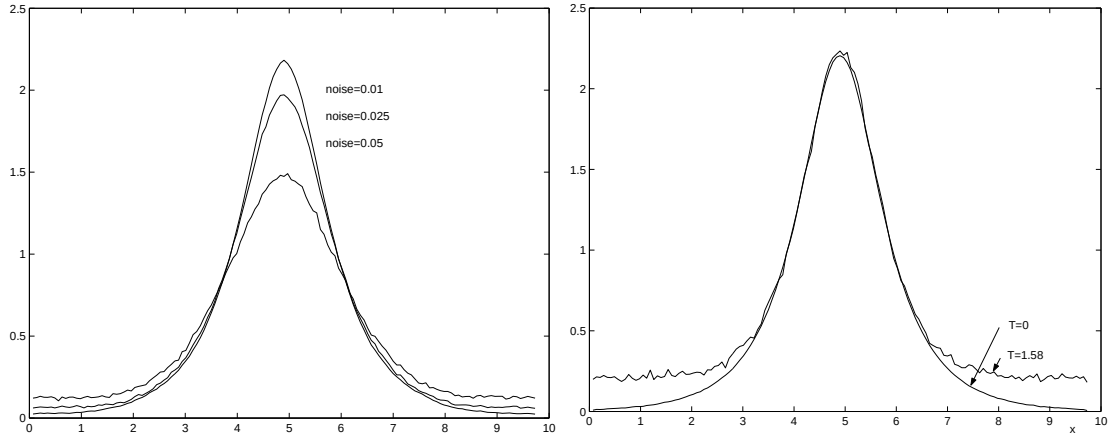

Figure 13: Sections of $< |u| >$ at $T = \pi/2$ for NLS with multiplicative noise ($\sigma = 1$, $\epsilon = 0.05,\ 0.025,\ 0.01$) on the left and additive noise ($\sigma = 1$, $\epsilon = 0.05$) on the right.

In figure 14, we show the evolution of $\mathbb{E}(\max_{x\in D} |u(t,x)|)$, the expectation of the maximum amplitude, for various levels of multiplicative noise and compare it to $\mathbb{E}(|u(t,x_c)|)$ for $\epsilon = 0.025$ - recall that $\mathbb{E}(|u(t,x_c)|)$ is a very good approximation of $\max_{x\in D} \mathbb{E}(|u(t,x)|)$. We see that again $\mathbb{E}(|u(t,x_c)|)$ monotonically decreases and $\mathbb{E}(\max_{x\in D} |u(t,x)|)$ increases first on a small interval of time. Thus the mechanism described above seems to work also in the critical case.

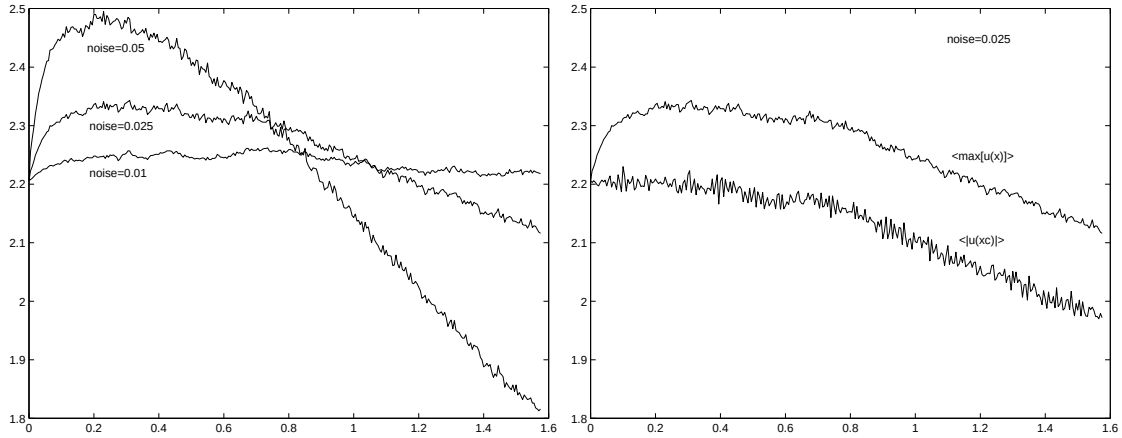

Figure 14: Evolution of the approximation of $\mathbb{E}[\max_{x\in D}|u(t,x)|]$ (left, $\epsilon = 0.05,\ 0.025,\ 0.01$) and $\mathbb{E}[\max_{x\in D}|u(t,x)|]$ and $\mathbb{E}|u(t,x_c)|$ (right, $\epsilon = 0.025$) for NLS with multiplicative noise ($\sigma = 1$).

In figure 14, we see that, for an additive noise, no damping can be detected on the evolution of $\mathbb{E}(|u(t,x_c)|)$. It may be too weak and a more precise simulation should be performed to see if it still exists.

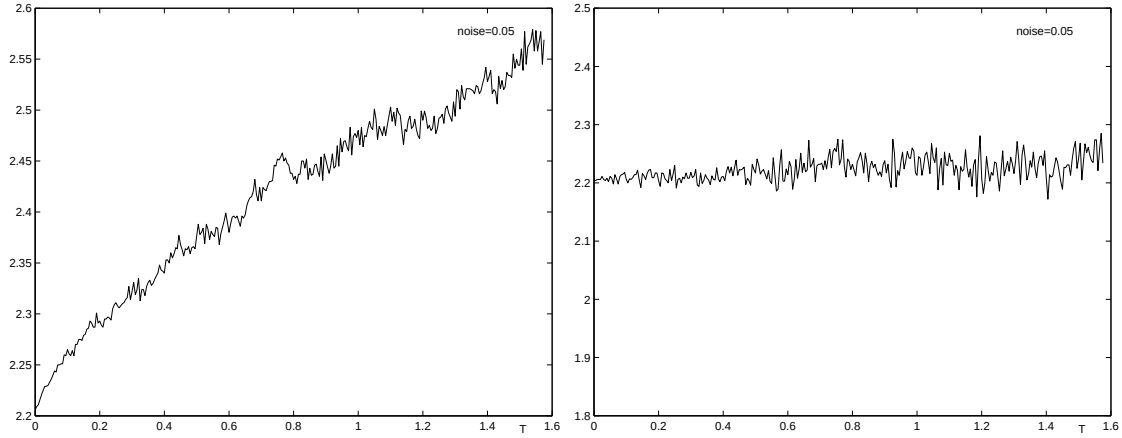

Figure 15: Evolution of the approximation of $\mathbb{E}[\max_{x\in D}|u(t,x)|]$ (left) and $\mathbb{E}|u(t,x_c)|$ (right) for NLS with additive noise, ($\sigma = 1$, $\epsilon = 0.05$).

3.3 Comparison of the damping effects with a diffusion

We have seen that a noise has a tendency to damp the solution. In the probabilistic vocabulary, the solution of a stochastic equation is also called a diffusion. This is related to the fact that the probability density evolves according to a parabolic equation. Thus this meaning of the word diffusion is totally different to what a diffusive term in an equation means. If we add such a diffusion to the NLS equation, we obtain the so-called complex Ginzburg-Landau equation (CGL). We intend now

to see if the damping due to the multiplicative noise is comparable to the damping due to a diffusive term. In other words, we compare the solutions of the NLS equation in the multiplicative case and the CGL equation,

$$\frac{\partial u}{\partial t} - (\mu + i)\Delta_d u + (\nu - i)|u|^{2\sigma} u = 0, \tag{10}$$

where μ and ν are small nonnegative parameters.

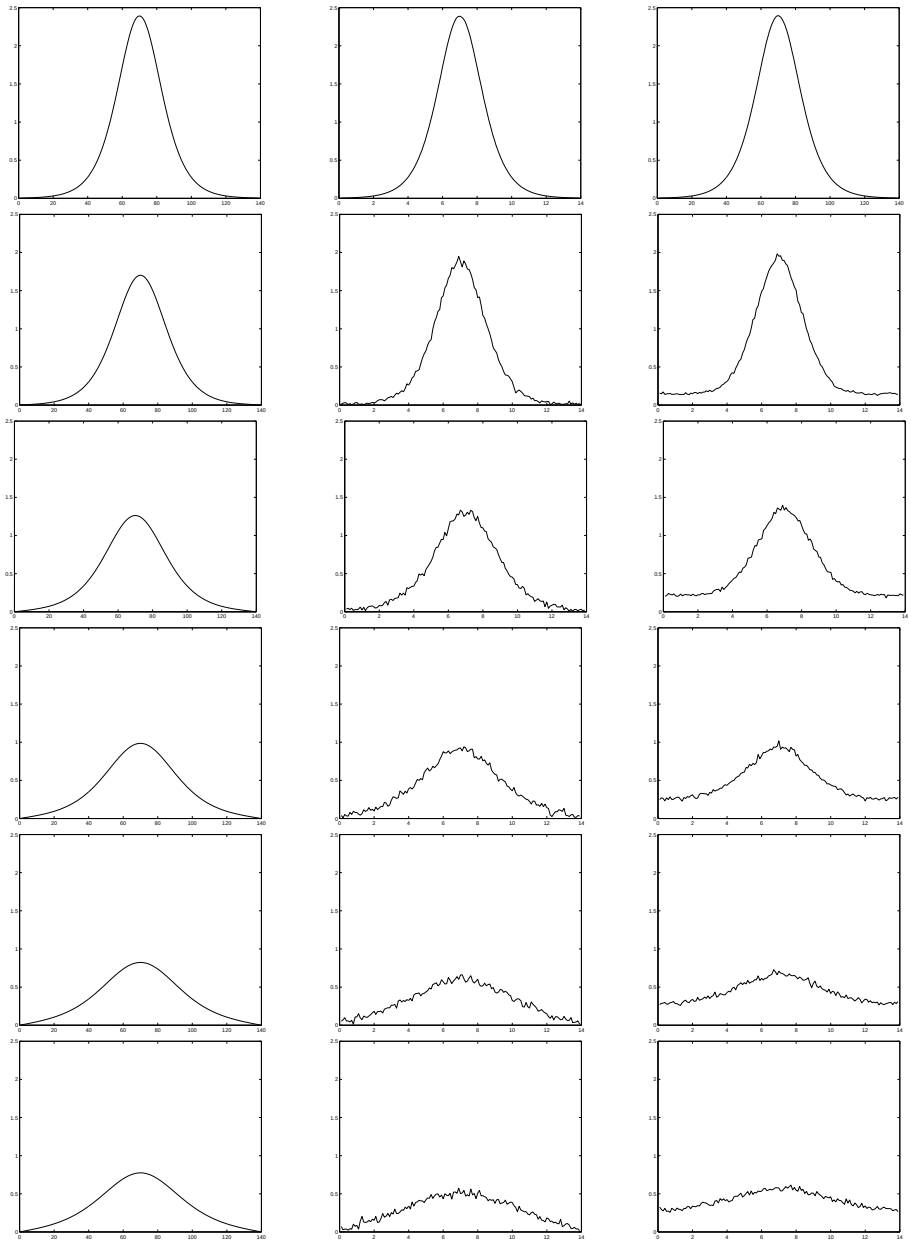

Figure 16: Comparison of the evolution of the sections of the solution for CGL ($\mu = \nu = 0.055$, left column) and NLS with multiplicative noise ($\epsilon = 0.05$): section of $| < u > |$ (center column) and section of $< |u| >$ (right column), for $t = 0,\ t = 2,\ t = 4,\ t = 6,\ t = 8,\ t = 9$ ($\sigma = 1$).

We compute solutions of (10) starting from the same Cauchy data as the one taken in stochastic simulations of NLS. We have chosen the various parameters , μ, ν, ϵ, so that the solution are as close as possible. The profiles of the CGL solution and of one path of the stochastic NLS with multiplicative noise at different times are shown in figure 16. The evolutions are very similar and the two effects could easily be confused. The superposition of the CGL and stochastic profiles in figure 17 is really amazing. We insist however that the two perturbations of NLS are mathematically completely different even if it seems difficult to see the difference on the solution behavior.

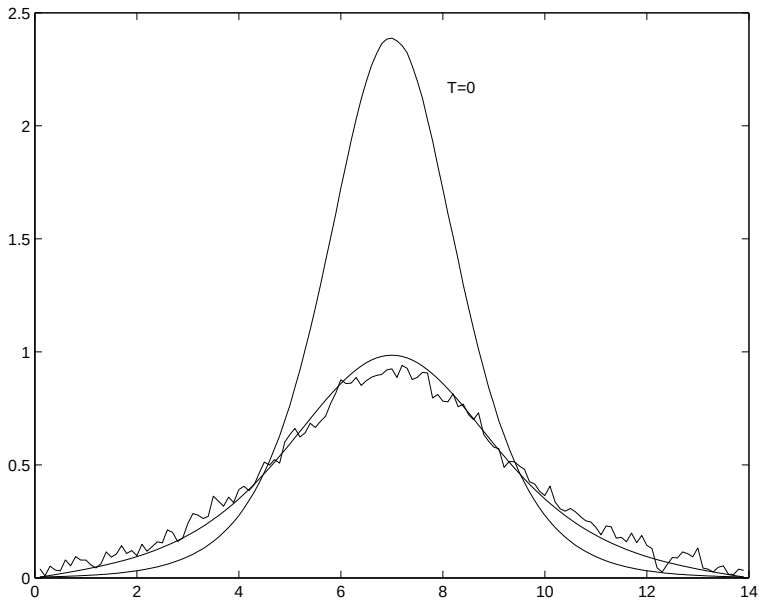

Figure 17: Sections of $< u >$ at $t = 0$ and $t = 6$ for NLS with multiplicative noise ($\epsilon = 0.05$) compared with CGL ($\mu = \nu = 0.055$).

Nevertheless, a slight difference can be seen on the evolution of the maximum amplitude (see figure 18): in the case of the multiplicative noise, an inflection point can be observed in the $< |u(t, x_c)| >$ evolution, whereas the evolution for the CGL equation mimics a dissipative profile. This difference is related to the fact that the stochastic NLS equation is conservative - the L^2 norm is conserved - whereas CGL equation is dissipative - the L^2 norm decreases.

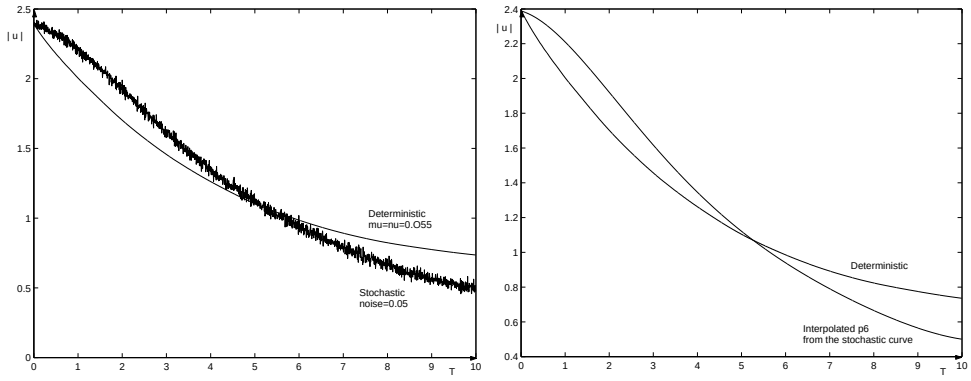

Figure 18: Comparison of the evolution of the maximum of the solution for CGL ($\mu = \nu = 0.055$) and $< |u(t, x_c)| >$ for NLS with multiplicative noise ($\epsilon = 0.05$), ($\sigma = \frac{1}{2}$, $\epsilon = 0/0.05$ $\mu = \nu = 0,\ 0.055$, $K = 0$).

4 Noise effect on the blow-up

4.1 The numerical study of singular solutions

As already mentioned, the computation of singular solution is delicate and requires a careful treatment. In [3] and [4] - see also [7], [8] for the Korteweg-de Vries equation - sharp criteria for refinement are derived. Let us first recall that it is absolutely necessary to refine the grid when computing a singular solution for the deterministic NLS equation. Indeed, the H_0^1 norm increases strongly whereas the L^2 norm remains invariant. This is in contradiction with the well known inverse inequality

$$\|u\|_{H_0^1} \leq \frac{C}{h}\|u\|_{L^2}, \tag{11}$$

valid for a discrete function u. Thus, if the grid is uniform, it is impossible to simulate blow-up.

Figure 20 shows the computed solution with and without refinement in the case of an initial data corresponding to a singular solution. Due to the inverse inequality, the maximum norm cannot reach high values and oscillates on the fixed grid. On the contrary, with refinement, the computed profile shows a singularity.

In the articles cited above, the refinement strategy is the following. The time step is divided by 2 when the energy conservation fails and the spatial refinement occurs when the inverse inequality is close to become false. This gives the following algorithm:

$$\text{if} \quad \|\nabla u^n\|_2 \geq c_1 \frac{C}{h}\|u^n\|_2, \quad \text{then add points in the grid,}$$

$$\text{if} \quad \frac{|H(u^{n+1}) - H(u^n)|}{|H(u^n)|} \geq c_2 \quad \text{then divide } \delta t \text{ by } 2,$$

where c_1 is a positive constant smaller than 1, C is the constant in (11), and c_2 is a positive constant close to 0. These have to be chosen in order to optimize the refinement algorithm. If c_1 and c_2 are small, the refinements are too frequent and yields prohibitive computational costs. In the worst case, if the time step is refined too often, the simulation cannot reach the blow-up time.

Moreover, a global space refinement would also need very long computational time. We observe that the solutions we are interested in remain localized near the center of the square and in order to improve our computations, we chose to refine locally in space. Indeed, it is no use having a refined grid in spatial areas where the solution is not singular. Since the singularity will always occur at the center of the domain, we chose a refinement procedure which adds points only around the center. Our refinement procedure consists in adding K points from the center to the left and K points to the right in x and in y directions. The refined grid has the shape of a centered cross. Figure 19 shows on the left the grid after the first refinement and on the right the grid after the second one. All lines intersections in this figure are nodes of computation. Another choice would be to add points only on a small centered square, this method has the advantage to refine only where the singularity appears and the refined grid has fewer points. However, the code would be much more complex to implement and the matrix M of our scheme (see Section 2.3) would loose its symmetry.

The refinement strategy described above cannot be applied with our scheme. Indeed contrary to [3] and [4], the energy is exactly conserved in our case and it cannot be used to decide when to refine. If the energy changes, this means that our fixed point algorithm does not converge and it is in general already too late to refine in time. Based on this observation, we have decided to refine in time when iterations in the fixed point is larger then a prescribed value. This criterium of time refinement gives good results in the deterministic case for NLS. Another advantage is that the fixed point and conjugated gradient are efficient resulting in a quite fast computation. Furthermore, this criterium is also available in the stochastic case or for the complex Ginzburg-Landau. In these two cases, no invariant quantity such as the energy exists. Concerning space refinement, we keep the criterium based on the inverse inequality.

It has to be emphasized that the matrix conditioning becomes worse and worse with the number of space refinement and the preconditioning is less and less efficient.

Another point is that, when the spatial grid is refined, it is necessary to choose values for the solution at the new nodes. A first try was to use linear interpolation. However, this produces a significant break in the evolution of the mass and energy. We have used interpolation with second order polynomials in order to cure this problem.

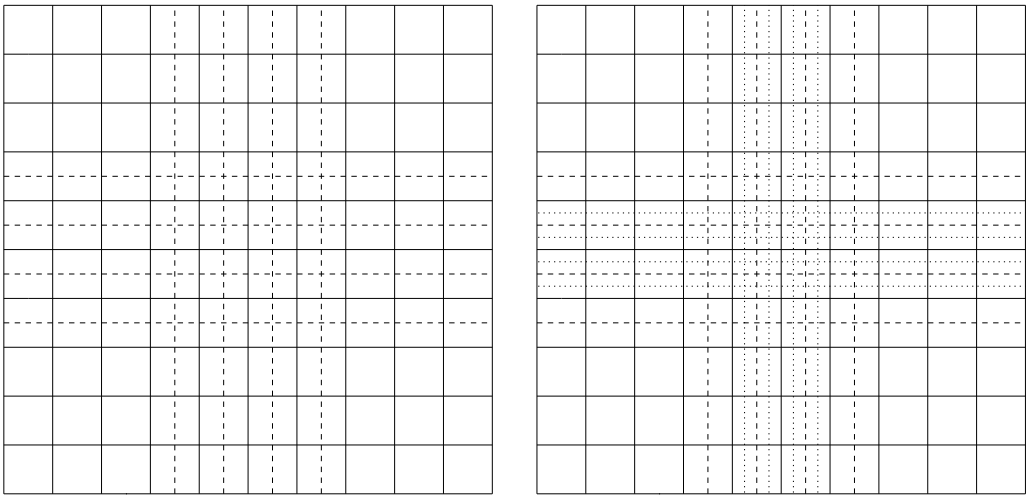

Figure 19: The grid 10×10 after one refinement with $K = 2$ (left) and after the second one (right).

The second solution shown in figure 20 has been computed with this strategy with $K = 20$. We see that our code is able to compute singular solution in a very efficient way. It is also important to make sure that the code is able to compute high amplitude solutions which finally decrease after a strong focusing phase. This may happen in the critical case for the complex Ginzburg-Landau equation. Indeed, it is known that the solutions are global (see [17]) but, for μ and ν small, they are very close to the NLS solutions. Consequently, for an initial data with negative energy, we expect to see numerically a solution very close to the blowing up solution of NLS, but which stays global in time.

Tests have been made in the critical case $\sigma = 1$ with a Gaussian initial condition

$$u_0(x, y) = qe^{-((x-7)^2+(y-7)^2)}, \tag{12}$$

with $q = 3$ so that it has a negative energy. We have taken $\mu = \nu$. The program is supposed to stop when the amplitude of the solution is 5000 times higher than the initial amplitude. The initial number of point in each direction is 140 and we prescribed $K = 20$. The domain is the square $[0, 14] \times [0, 14]$. When $\mu = \nu = 10^{-2}$ or $\mu = \nu = 10^{-3}$, we indeed obtain a solution which first focuses. Then the diffusion dominates and the amplitudes decreases. In the second case, we could believe from the figure on the left that the solution is singular but the zoom on the right shows that it is not not the case. For $\mu = \nu = 10^{-4}$ the amplitude of the solution goes over the limit of $5000\, q$, and no stopping effect of the blow up was numerically established. More severe refinement criteria would show that the solution is global. This shows that one has to be very careful before concluding that a solution is singular ! In our situation, we can only conclude that there is a threshold between $\mu = \nu = 10^{-3}$ and 10^{-4} and below this threshold no global solution could be numerically seen although we know it exists.

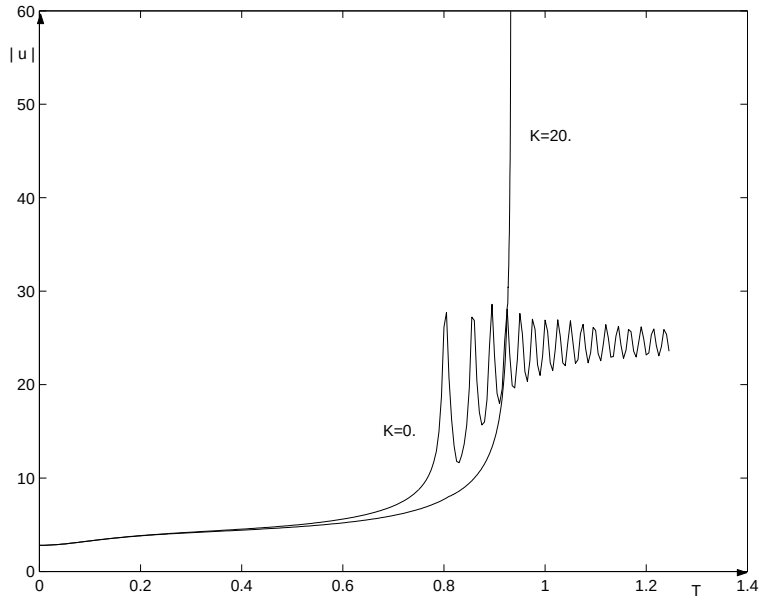

Figure 20: Comparison of the evolution of the maximum of a blowing-up solution for critical NLS with refinement ($K = 20$) and without refinement ($K = 0$).

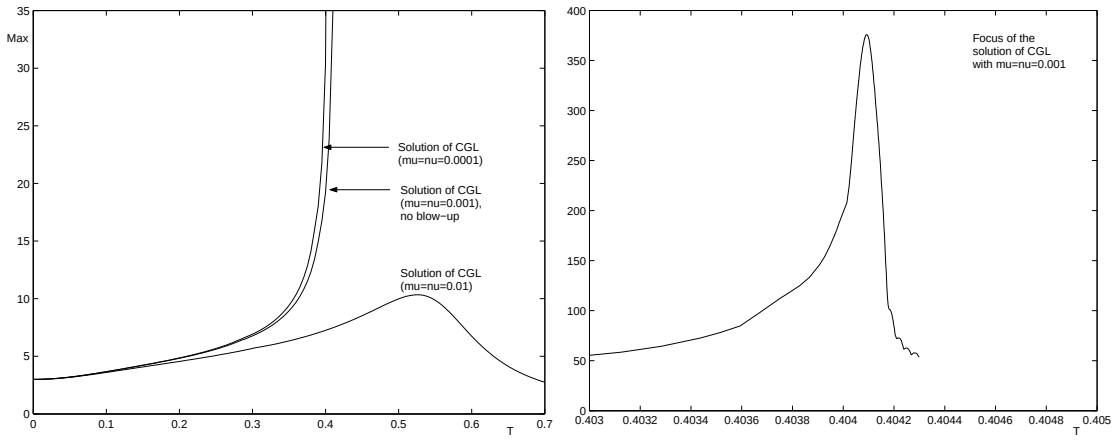

Figure 21: Amplitude profile of CGL solutions with negative initial energy for different μ and ν ($\mu = \nu = 0.0001,\ 0.001,\ 0.01$, $\sigma = 1$, $q = 3$, $\epsilon = 0$, $K = 20$).

We now turn our attention to the stochastic case. We believe that the deterministic criteria are still good to capture a singular solution in the presence of noise. Moreover, as shown in [15], refinement is also necessary to get a correct discretization of a white noise. A noise discretized on a grid with a fixed mesh size cannot be white. Its correlation length is of order of the mesh size. Since blow-up is a phenomenon where all frequencies are important, a space correlated noise cannot have a strong effect on this mechanism. If we want to understand the influence of a space

time white noise on blow-up, it is necessary to have arbitrarily small space and time step.

We encountered new difficulties in the stochastic case. First, we had to choose a larger constant c_1. Indeed, the H^1 norm increases due to the presence of noise and, if c_1 is too small, this yields unnecessary spatial refinements.

Another problem appeared. As mentioned previously, the condition number of the matrix is worse and worse with the number of refinements. In the presence of noise the number of iterations in the conjugate gradient algorithm can reach very high values, as opposed to the deterministic case. The reason is that, for deterministic evolution problems, the solution is rather smooth in time and the conjugate gradient is initialized with a vector close to the solution so that the convergence is very fast. However, this is no more the case in the stochastic case where the solution is not very smooth in time so that u^{n+1} is often very different from u^n and the convergence of the conjugate gradient may be very long. We have chosen to refine in time also in this case, when the number of iterations in the conjugate gradient is too large. This might be bad and lead to very long computations. However, we found that it was a good solution and could always perform our simulations in a reasonable time.

4.2 Numerical simulations

All the simulations are done according to the algorithm described above on the square $[0, 14] \times [0, 14]$ with a critical nonlinearity. We will start our study of blow-up with the Gaussian initial condition (12), where q is such that $H(u_0)$ is slightly negative or slightly positive but we know that the deterministic solution is singular. We will also use the deterministic stationary wave as initial condition, due to instability the deterministic numerical solution is also singular.

For $q = 3$, the Gaussian initial data has negative energy. Figure 22 on the left displays a path of the solution for two noise levels, $\epsilon = 0.1$ and 0.05. The blow-up is prevented with the high noise level whereas it still occurs for $\epsilon = 0.05$. However, we believe that this is a numerical artefact and that in fact the stochastic solution is not singular. Recalling the deterministic simulation on the complex Ginzburg-Landau equation, we know that this is possible. An indication of that is that if we do more and more refinement, *i.e* if we take c_1 smaller and smaller, the blow-up is delayed, which means that our simulations have not converged. However, even with very severe refinement criteria, we have not been able to establish that the stochastic solution is global. Note that we tried several random draws and each time we observed the same behavior.

We tried to see for which level level of noise we are able to establish that the stochastic solution does not develop singularities. In figure 23, we see that up to $\epsilon = 0.08$ the blow-up is always prevented. With this noise level, the solution starts to focus very strongly but the refinement algorithm works well, the noise is very close to a space time white noise around the maximum and the blow-up does not occur. Below this level, we have not been able to obtain this behavior.

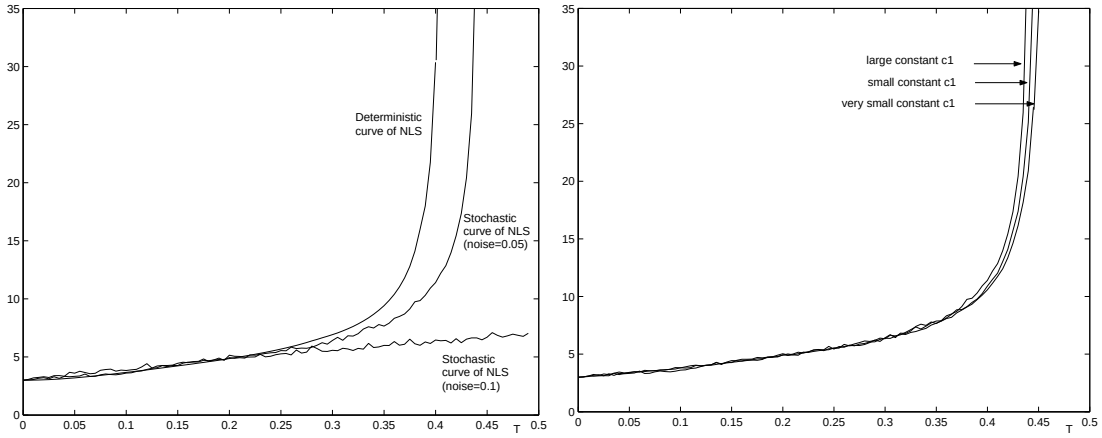

Figure 22: Profile of the solution amplitude of NLS with multiplicative noise ($\epsilon = 0.05,\ 0.1$) compared to the deterministic blow-up (left) and profile of the solution amplitude of NLS with multiplicative noise ($\epsilon = 0.05$) for 3 different constants c_1 (right) ($\sigma = 1$, Gaussian initial data ($q = 3$), $K = 20$).

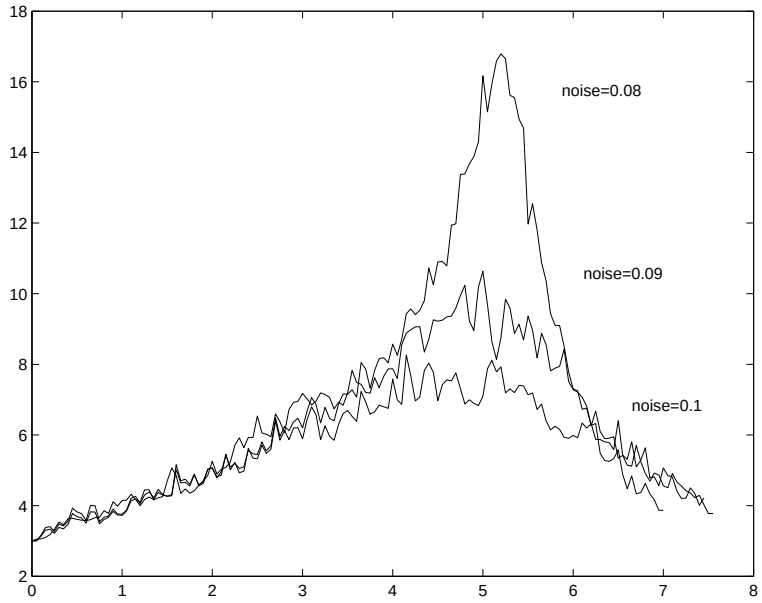

Figure 23: Profile of the solution amplitude of NLS with multiplicative noise with various noise level.

We then choose the initial data (12) with $q = 2.8$ that gives a blowing up solution with a positive energy. In this case, the noise influence is easier to observe since the deterministic blow-up is weaker. Our experiments have shown that collapse is stopped when ϵ is larger than 2.10^{-2}. Indeed for $\epsilon = 3.10^{-2}$, which is quite small, the blow-up is early stopped. In fact, there was not even one refinement in this case. For $\epsilon = 2.5.10^{-2}$, the blow-up is stopped after a high peak of amplitude (see Figure

24). In this latter case, the refinement method is necessary to observe the global solution. Even for $\epsilon = 2.0.10^{-2}$, the solution amplitude becomes very large but the blow-up is still prevented. A focus on the solution near the singularity confirms that the decreasing of the amplitude is not due to a numerical instability. We indeed see in Figure 25 (right) that the computation is good and that there is a real damping effect that occurs in a very short time scale. Under the critical level $\epsilon = 2.10^{-2}$, no global solution could be seen numerically.

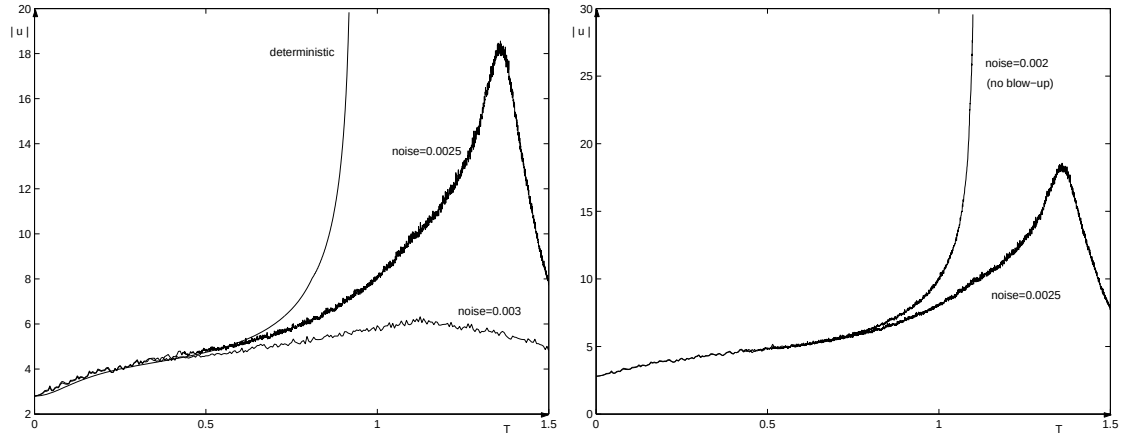

Figure 24: Profile of solution amplitude of NLS with multiplicative noise for different ϵ ($\sigma = 1$, Gaussian initial data with positive energy ($q = 2.8$), $K = 0$).

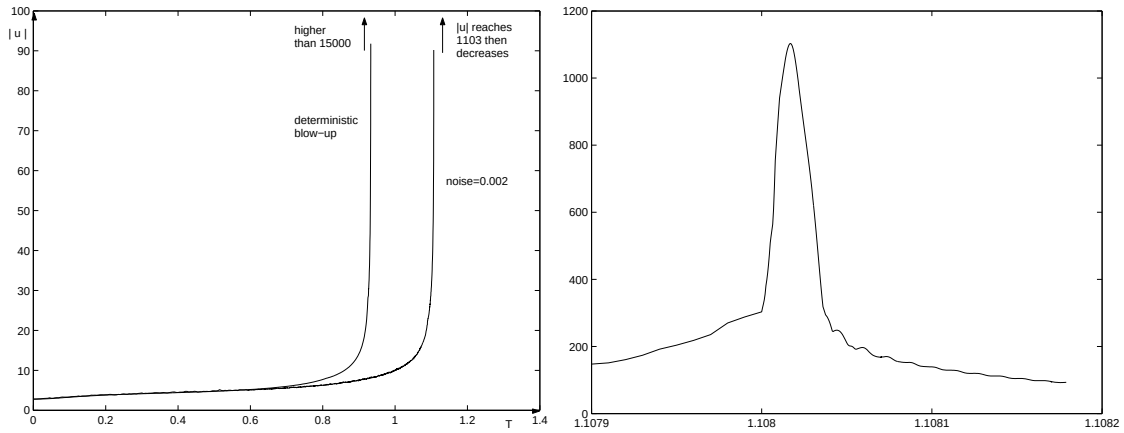

Figure 25: Profile of solution amplitude of NLS with multiplicative noise ($\epsilon = 0.02$) compared to the deterministic blow-up (left) and zoom around maximum intensity for $\epsilon = 0.02$ (right). ($\sigma = 1$, Gaussian initial data with positive energy ($q = 2.8$), $K = 20$).

Finally, we consider the stationary wave described in Section 3 as initial condition. The solution is not stable and numerically blows up after some time, see figure

26 (left). In this case, the blow-up is very weak and easily prevented by the multiplicative noise, even if ϵ is very small, see figures 26 and 27. Besides for $\epsilon \geq 6.10^{-4}$, no refinement procedure is necessary since the stationary wave is really early prevented. Nevertheless, for $\epsilon = 5.10^{-4}$, a severe focusing happens and the local space refinement procedure is necessary to see the damping effects of the noise on the blow-up. For smaller noise level, $\epsilon < 5.10^{-4}$, no global solution could be observed. As in the previous cases, we cannot really conclude whether there is still a global solution or not because our computation reaches its limit. However, we firmly believe that even if we cannot see it in the simulations for very small ϵ, the solution is always global with multiplicative white noise for any value of the noise level ϵ.

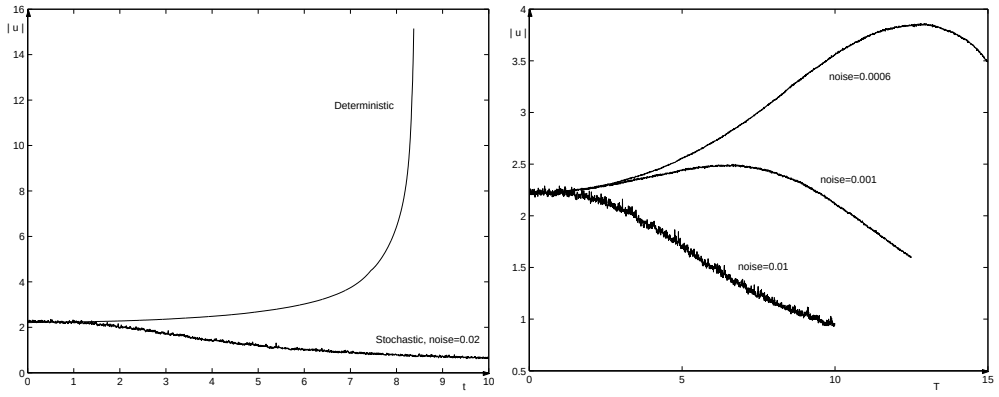

Figure 26: Evolution of the solution amplitude of NLS with multiplicative noise for different ϵ ($\sigma = 1$, stationnary state, $K = 0$).

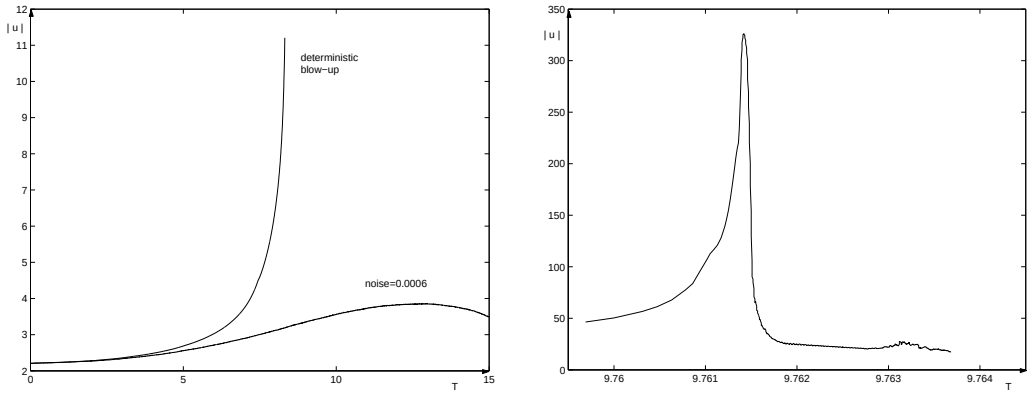

Figure 27: Evolution of the solution amplitude of NLS with multiplicative noise for small ϵ compared to the deterministic solution ($\sigma = 1$, stationary state, $K = 0$) (left) and zoom of the solution amplitude for the critical value of $\epsilon = 5.10^{-4}$ (right).

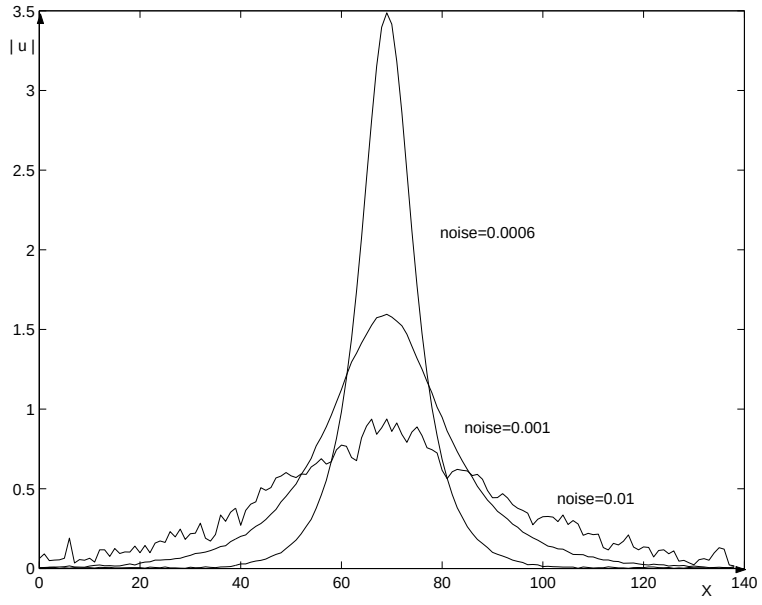

Figure 28: Final section of the solution for different ϵ (critical Schrödinger unstable stationnary state, $\sigma = 1$, $K = 0$).

It is surprising that a very small noise can drastically change the solution behavior although it is difficult to detect. We can see on figure 29 the evolution of the solution with the noise level $\epsilon = 6.10^{-4}$. The noise is not visible on the profile but it is strong enough to prevent the blow-up. A closer look at the profile is shown in figure 28. We see that, contrary to the case of larger values of ϵ, it is very difficult to detect the noise.

We conclude that with a small noise it is possible to have a propagation for a much longer time compared to the deterministic case. However, due to the damping effect of the noise, the wave disappears progressively. If we consider that the propagation is destroyed if the amplitude has been divided by two, we can compute the life time of the wave as a function of the noise level. The corresponding curve is shown in figure 30. We can see that, above a very small limit, the smaller ϵ is, the longer the life time of the wave is. Table 1 shows that the L^2 norm is very weakly dissipated. Thus, the blow-up is really prevented by the noise and not by the numerical dissipation of the scheme.

Time	0	2	4	6	8	10	12	14	16
L^2 norm	11.7	11.68	11.66	11.64	11.6	11.57	11.54	11.5	11.48

Table 1: Evolution of the L^2 norm for $\epsilon = 6.10^{-4}$.

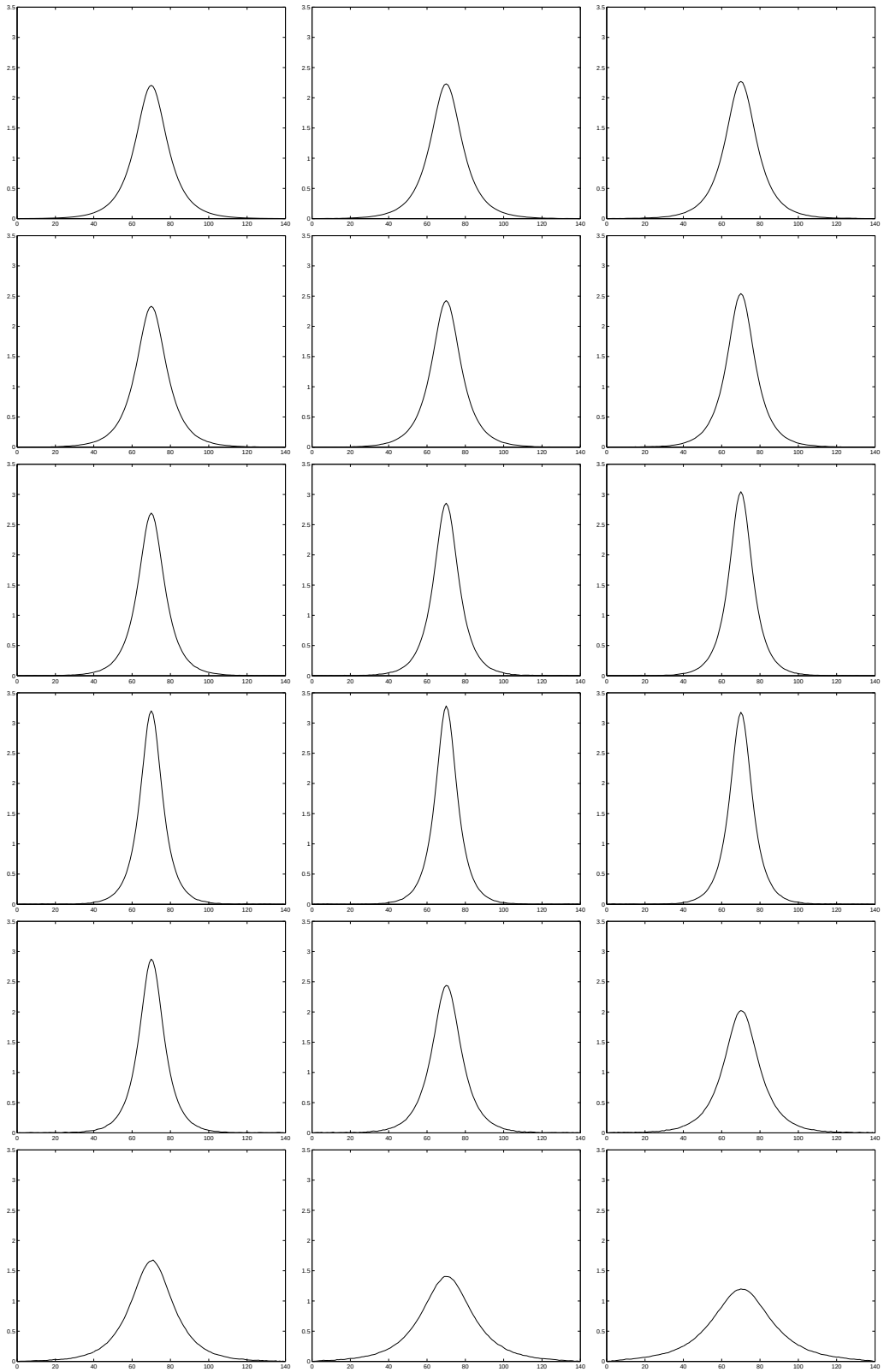

Figure 29: Evolution of the sections of the stationary unstable solutions in the critical case with multiplicative noise ($\epsilon = 0.006$), from $T = 0$ to $T = 17$.

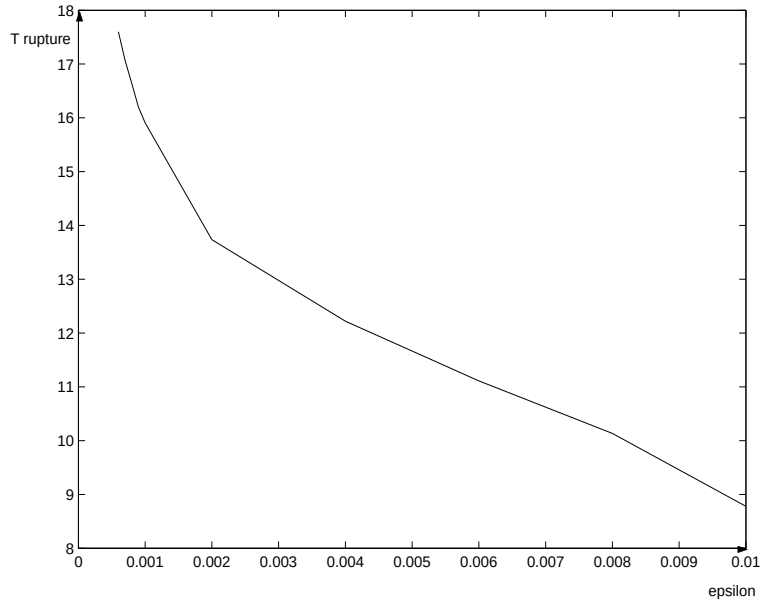

Figure 30: The stationary wave life time with respect to ϵ.

References

[1] F. Kh. Abdullaev, S. Darmanyan and P. Khabibullaev, Optical solitons, Springer Series in Nonlinear Dynamics (1993).

[2] F. Kh. Abdullaev and J. Garnier, Solitons in media with random dispersive perturbations, Physica D 134, 303-315 (1999).

[3] G. D. Akrivis, V. A. Dougalis, O. A. Karakashian and W.R. McKinney, Galerkin finite element methods for the nonlinear Schrödinger equation, Hellenic research in mathematics and informatics 92 (Athens 1992) 421-442, Hellenic Math. Soc., Athens (1992)

[4] G. D. Akrivis, V. A. Dougalis, O. A. Karakashian and W. R. McKinney, Numerical approximation of singular solutions of the damped nonlinear Schrödinger equation, ENUMATH97 (Heidelberg), 117-124, World Sci. Publishing, River Edge, NJ (1998).

[5] O. Bang, P.L. Christiansen, F. IF and K. Rasmussen, and Y.B. Gaididei, White noise in the two dimensional nonlinear Schrödinger equation, Appl. Math. 57, 3-15 (1995).

[6] M. Barton-Smith, Etudes numériques et théoriques sur les équations de Schrödinger et Ginzburg-Landau complexe stochastiques, Ph. D Thesis, Paris-Sud Orsay University, 7111, 2002.

[7] J. L. Bona, V. A. Dougalis, O. A. Karakashian and W. R. McKinney, Computations of blow-up and decay for periodic solutions of the generalized Korteweg-de-Vries-Burgers equations, A Festschrift to honor Professor Garrett Birkhoff on his eightieth birthday. Appl. Numer. Math. 10 n. 3-4, 335-355 (1992).

[8] J. L. Bona, V. A. Dougalis, O. A. Karakashian and W. R. McKinney, Numerical simulation of singular solutions of the generalized Korteweg-de-Vries equation, *Mathematical problems in the theory of water waves (Luminy, 1995)* 17-29, Contemp. Math., 200, Amer. Math. Soc., Providence, RI (1996).

[9] H. Brezis and T. Gallouet, Nonlinear Schrödinger evolution equations, Nonlinear Analysis TMA 4 n. 4, 677-681 (1980).

[10] T. Cazenave, An Introduction to Nonlinear Schrödinger equations, *Textos de metodos matematicas,* 26. Instituto de Matematica - UFRJ - (1996).

[11] A. de Bouard and A. Debussche, The stochastic nonlinear Schrödinger equation in H^1, Stochastic Analysis and Applications, vol. 21, n. 1, p. 97-126, (2003).

[12] A. de Bouard and A. Debussche, On the effect of a noise on the solutions of focusing supercritical nonlinear Schrödinger equation, Prob. Theory Related Fields 123 n. 1, 76-96 (2002).

[13] A. de Bouard and A. Debussche, Semi-discrete scheme for the stochastic nonlinear Schrödinger equation, Numer. Math., 96, n. 1, (2003).

[14] A. de Bouard and A. Debussche, Blow-up for the stochastic nonlinear Schödinger equation with multiplicative noise. Preprint IRMAR, 03-02, Université de Rennes 1.

[15] A. Debussche and L. Di Menza, Numerical simulation of focusing stochastic nonlinear Schrödinger equations, Physica D 162 n. 3-4, 131-154 (2002).

[16] A. Debussche and J. Printems, Numerical simulation of stochastic Korteweg-de Vries equations, Phys. D 134, 220-226 (1999)

[17] C.R. Doering, J.D. Gibbon and C.D. Levermore, Weak and strong solutions for the complex Ginzburg-Landau equation, Physica D, vol. (1994) 285-318.

[18] G.E. Falkovitch, I. Kolokolov, V. Lebedev and S.K. Turitsyn, Statistics of soliton-bearing systems with additive noise, Phys. Rev. E 63, 025601(R) (2001).

[19] J. Garnier, Asymptotic transmission of solitons through random media, SIAM J. Appl. Math. 58 n. 1, 1969-1995 (1998)

[20] R.T. Glassey, On the blow-up of solutions to the Cauchy problem for nonlinear Schrödinger equations, J. Math. Phy. 18, 1794-1797 (1977).

[21] F. Ivanauskas, On convergence of difference schemes for nonlinear Schrödinger equations, the Kuramoto-Tsuzuki equation and systems of reaction diffusion type systems, Liet. Math. Rink., 34 (1994), 32-51.

[22] O. Kavian, A remark on the blowing-up solutions to the Cauchy problem for nonlinear Schrödinger equations, Trans. Amer. Math. Soc. 299 n.1, 193-203 (1987).

[23] V. Konotop and L. Vazquez, Nonlinear random waves, World Scientific Publishing Co., Inc, River Edge, NJ 1994.

[24] G.N. Milstein, Y.P. Repin and M.V. Tretyakov, *Mean-square symplectic methods for Hamiltonian systems with multiplicative noise*, Preprint, Berlin, 2001.

[25] J. Printems, Aspects théoriques et numériques de l'équation de Korteweg-de Vries stochastique, Ph. D., University Paris-Sud Orsay.

[26] M. Radziunas, On convergence and stability of difference schemes for nonlinear Schrödinger type equations, Liet. Math. Rink., 36 (1996), pp. 224-244.

[27] K. Rasmussen, Y. B. Gaididei, O. Bang and P. L. Christiansen, The influence of the noise on critical collapse in the nonlinear Schrödinger equation, Phys. Rev. A 204, 121-127 (1995).

[28] J. C. Scalerandi, A. Romano and C. A. Condat, A Korteweg-de Vries solitons under additive stochastic perturbations, Phys. Rev. A 204, 121-127 (1995).

[29] P. L. Sulem and C. Sulem, The nonlinear Schrödinger equation, self-focusing and wave collapse, AMS, Springer-Verlag, 1999.

[30] P.L. Sulem and C. Sulem, Focusing nonlinear Schrödinger equation and wave-packet collapse, (Proceeding of the Second World Congress of Nonlinear analysts, Part 2, Athens, 1996), Nonlinear Anal. 30 n. 2, 833-844 (1997).

[31] P. L. Sulem and C. Sulem, The Focusing nonlinear Schrödinger equation: effect of the coupling to a low frequency field, Math. Comput. Simulation 43 n. 1, 57-66 (1997).